Exploring the Possibility of Low Temperature Glazing in Faience from the Djoser Step Pyramid through Compositional Analysis

by

Lawrence A. Whisenant

Submitted to the Department of Materials Science and Engineering in Partial Fulfillment of the Requirements for the Degree of

Bachelor of Science

at the

Massachusetts Institute of Technology

June 2012

Signature of Author: _____
Department of Materials Science and Engineering
May 11, 2012

Certified by: _____
Linn Hobbs
Professor of Materials
Professor of Nuclear Engineering
Thesis Supervisor

Accepted by: _____
Jeffrey Grossman
Carl Richard Soderberg Professor of Power Engineering
Chair, Undergraduate Committee

Exploring the Possibility of Low Temperature Glazing in Faience from the Djoser Step Pyramid through Compositional Analysis

by

Lawrence A. Whisenant

Submitted to the Department of Materials
Science and Engineering on May 11, 2012
in Partial Fulfillment of the Requirements
for the Degree of Bachelor of Science
in Archaeology and Materials

Abstract

Egyptian faience, a glazed, non-clay based ceramic material, is found throughout Egypt in a time range pre-dating the Predynastic Period (5500 – 3100 BCE) and extending well beyond the Roman Period (30 BCE – 641 CE). One of the most monumental feats of faience production and one of the first examples of mass production in human history is the collection of approximately 36,000 faience tiles from the Step Pyramid of the Third Dynasty Pharaoh Djoser (2667 – 2648 BCE).

Based on past research, these tiles have been supposed to be glazed in a range of firing temperatures from 850°C to 900°C. Recent research of efflorescence-glazed tiles has introduced the possibility that the tiles from Djoser's Step Pyramid may have been glazed at far lower temperatures between 250°C and 350°C, possibly due to the phosphorus content of the tiles.

The non-destructive analysis of a tile from the Djoser Step Pyramid, reported in this thesis, has yielded results using methods of x-ray fluorescence, environmental scanning electron microscopy, x-ray energy dispersive spectroscopy, x-ray diffraction and micro-computed tomography. It appears that the tile was glazed by the method of "application." There is evidence that may support hypotheses of low temperature glazing, though the phosphorus content of the faience core and of the glaze does not fully explain the phenomena.

Thesis Advisor: Linn Hobbs
Title: Professor of Materials and Professor of Nuclear Engineering

Index of Figures

Index of Tables

Historical Background

Defining Egyptian Faience

Egyptian faience, in modern scientific terms is a glazed, non-clay-based ceramic (Nicholson and Peltenburg 2000). Instead, the core of this material is primarily composed of fine, crystalline quartz held together by a glassy phase in the core. The core is covered with a colorful glaze, most notably blue turquoise in color, the appearance of which is determined by the type and amount of transition metal it contains (Kiefer and Allibert 1971; Tite 1987). In some cases, objects made of this material contain limited amounts of either lime and natron (a natural mixture of mostly sodium carbonate decahydrate ($Na_2CO_3 \cdot 10H_2O$) found in dry riverbed residues) or plant ash (Nicholson and Peltenburg 2000). Today, Egyptian faience can be found in sites from Mesopotamia and Pakistan to Scotland, as seen in Figure 1 (excluding Scotland). It is thought that this widespread

Figure 1: Map of geographical range of discovered faience artifacts (Frame, *et al.* 2010).

material was locally produced with material accessible in the environment (Nicholson and Peltenburg 2000).

To the ancient Egyptians, the non-clay-based ceramic was known as *thnt* (tjehenent) (Vandiver and Kingery 1986; Nicholson and Peltenburg 2000). This word, while meaning "faience," was also used to denote glass and otherwise glasslike materials (i.e. those similar in property to Egyptian faience). Though not used as frequently as *thnt*, the word *hsbd (khesbedj)* was sometimes used to refer to Egyptian faience (Vandiver and Kingery 1986; Nicholson and Peltenburg 2000). Meaning lapis lazuli (an example of which is seen in Figure 2), an often blue, semi-precious stone consisting mostly of

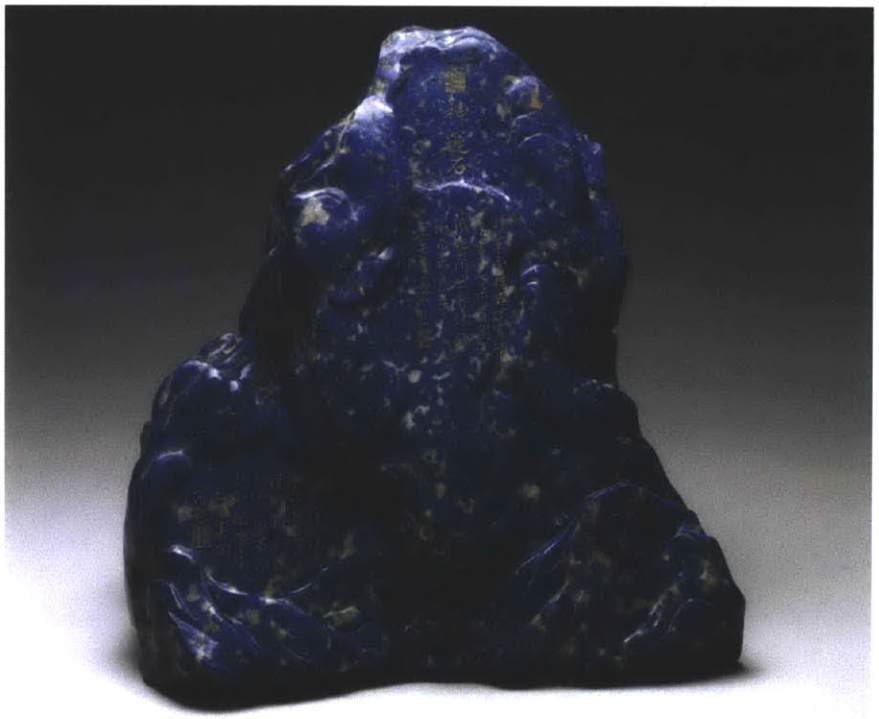

Figure 2: A sample of lapis lazuli from Taiwan (National Palace Museum 2012).

silicates, deposits of which are not found in Egypt, *hsbd* was also an Egyptian word for "blue," the most prestigious color to the ancient Egyptians (Vandiver and Kingery 1986). With these connections to prestige and power, large quantities, on the order of 30,000

Egyptian faience artifacts in the form of tiles were used in the burial chamber of the Step Pyramid (2667 – 2648 BCE), the tomb of the Third Dynasty Pharaoh Djoser of Upper and Lower Egypt (Vandiver and Kingery 1986). In addition, *thnt* and *hsbd* were related to the Egyptian words meaning "shining," "gleaming," or "dazzling," all of which describe Egyptian faience in its role as an artificial gemstone (Nicholson and Peltenburg 2000).

History of Production

Egyptian faience production involved a robust technology, present and changing from the Predynastic Period (5500 – 3100 BCE) until the Roman Period (30 BCE – 641 CE) and enduring in various forms through to the present without interruption (Nicholson and Peltenburg 2000; Kiefer and Allibert 1971). During this long history (over 3,000 years), the technology was subject to many changes. As society's view of the material and its cultural context changed and developed, so did the manufacturing processes behind its development. From vast experimentation to vast geographic distribution, Egyptian faience was a defining technology of ancient Egypt with an extensive history.

How did Egyptian faience and the culture surrounding it change from the Predynastic Period to the Roman Period? It is thought that early in the Predynastic Period, faience-like objects were produced in two ways. The first method involved working stone (e.g., by carving or abrading) into the desired form, then applying a glaze. The second method involved the use of a core primarily composed of silica. In the latter case, the cores were produced by modifying and shaping the raw materials (e.g., by modeling or the use of molds) into the desired forms. In reality, glazes are not as bright on natural stone as they are on processed materials, such as worked stone or crushed silica. Because of this

difference, there is the notion that the choice of processing was one made in favor of brightness and aesthetics (Nicholson and Peltenburg 2000).

How the glaze was applied during this period remains unsolved among three candidates: application glazing, efflorescence and cementation (Tite and Bimson 1986; Davidovits and Davidovits 2004). Application glazing involves applying the glaze in a liquid or powder form to the core of the object before firing. Efflorescence glazing involves the use of salts within the body of the object that are deposited on the surface (or effloresced) from the body during firing. Cementation glazing, the final method, involves introducing the glaze as a solid, in the form of a powder. The powder envelops the core of the object, composed of crushed silica, as it is fired. Of the three, application glazing seems the most likely to have been used during the Predynastic Period. Glazing via efflorescence is not supported by evidence prior to the Middle Kingdom.

Most of the faience objects from the Predynastic Period are quite small, like the beads in Figure 3. Beads constitute a significant portion of the faience objects known from this period (Nicholson and Peltenburg 2000). The introduction of beads as possible imitations of lapis lazuli and turquoise can be considered as the first of two major developments in faience production (Vandiver and Kingery 1986). As evidence for having been produced during a period of experimentation, the compositions of these bead- to amulet-sized artifacts are spread over a wide range. In fact, through studies of graves from cemeteries in Naqada and Tarkhan in Egypt, it has been demonstrated that the composition of artifacts can vary widely among objects found within a single grave. Some artifacts also point to a collaboration between faience workers and other artisans, such as goldsmiths;

Figure 3: Egyptian faience beads (ca. 3500 BCE) (Crew, Peltenburg and Spanou 2002).

faience has been found in a paste-form underlying a gold foil (Nicholson and Peltenburg 2000).

The Early Dynastic Period (3100 – 2686 BCE) yields artifacts, like those in Figure 4, that are larger than those found in the Predynastic Period. Detailed, small figurines as well as vessels made from faience are added to the faience repertoire.

Figure 4: *left:* shawabti (ca. 525-380 BCE); standing Horus (1567-1087 BCE); shawbati (ca. 1079-715 BCE); shawabti of a man named Zedher (ca. 380-343 BCE) (Curators of the University of Missouri 2012).

Except for one monumental endeavor, it was previously believed that faience production experienced a lull during the Old Kingdom (2686 – 2181 BCE). At Saqqara the Pharaoh Djoser of the Third Dynasty rests in the Step Pyramid. Within the pyramid complex are 36,000 mass-produced Egyptian faience tiles, some of which can be seen in Figure 5. The methods of producing these tiles are still under investigation. Lauer (Nicholson and Peltenburg 2000) has described the tiles as being formed from a mold, while Vandiver (Nicholson and Peltenburg 2000) has proposed a technique of "controlled forming," i.e., "rolling the paste between two parallel sticks in order to control the thickness and length but leaving the width to vary (Nicholson and Peltenburg 2000: 179)." Whichever method of molding was used, the tiles from the Step Pyramid are the earliest known examples of the utilization of molding for a monumental project. The introduction of molding to form objects from faience can be considered the second major development in faience production (Vandiver and Kingery 1986). The backs of the tiles

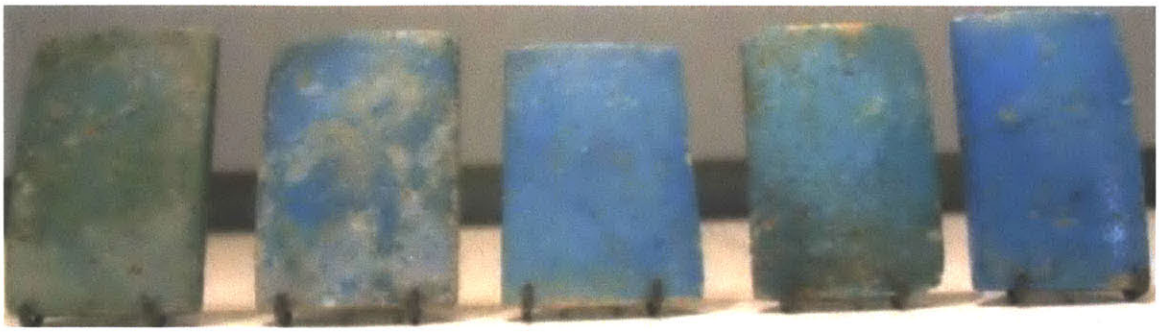

Figure 5: Faience tiles from the Djoser Step Pyramid (Davidovits and Davidovits 2004).

exhibit very little glaze, and such tiles are believed to have been glazed by the efflorescence method. Based on Vandiver's (Nicholson and Peltenburg 2000) 1983 study of Egyptian faience, all objects from the Early Dynastic Period through the First Intermediate Period (2181 – 2055 BCE), which were examined to determine the method of glazing, are thought to have been glazed by efflorescence. During this same span of time, the emphasis of experimentation and development was placed on methods of shaping rather than on glazing (Nicholson and Peltenburg 2000).

During the First Intermediate Period, Egypt saw a continuation of several endeavors, including the production of faience, but it lacked monumental endeavors, such as building the Step Pyramid, which were present in the Old Kingdom. During this time, Upper and Lower Egypt were not unified, and there is little historical evidence from this period in general (British Museum). Though politically restless, the First Intermediate Period still produced its fair share of Egyptian faience, as evidenced by the faience workshop at Abydos, the earliest example we have of such a workshop. This site is quite close to a temple from the Early Dynastic Period honoring the Egyptian god Khentiamentiu (a jackal-headed deity often associated with Anubis). The area is described as possessing circular features, possibly the remains of kilns. Some of these

features possess a broken-brick lining. Based on the ash lenses present, they are thought to have been used several times. Without a superstructure, as is believed to be the case, these possible kiln remnants may also be considered pits underlying bonfires used for open firing, a technique documented from pottery manufacture ethnographies. In the case of Egyptian faience, utilization of such "pit kilns" for firing would have required adjustments, particularly for the small bead-like objects that needed to be shielded from surrounding burning and burnt materials. Though it is almost certainly known that faience was produced at Abydos during this time, how the faience industry was organized and what purpose the production served are not known. The workshop's proximity to the Temple of Khentiamentiu may suggest a religious association (Nicholson and Peltenburg 2000).

The next periods of great diversity and experimentation occurred during the Middle Kingdom (2055 – 1650 BCE) and Second Intermediate Period (1650 – 1550 BCE). Though faience production was not halted by the political uncertainty of the First Intermediate Period, the stability brought by the Middle Kingdom may have served as a catalyst for the industry. The Middle Kingdom saw the production of thick-walled vessels, on which newer processing methods can be seen, such as the addition of a layer of fine quartz to the coarse body of the vessel to produce a vivid, bright glaze, an example of which can be seen in Figure 6 (Nicholson and Peltenburg 2000).

Figure 6: Hippopotamus (ca. 1961-1878 BCE) (Metropolitan Museum of Art 2012a).

Other developments during this time focused on the decoration of faience. The signature blue turquoise color was at its most intense during the Middle Kingdom, and this color preference extended into the New Kingdom (Kiefer and Allibert 1971). A marbled effect became more common as faience workers experimented more with the mixing of differently colored glaze pastes. In addition, darkly painted linear designs became a feature on blue backgrounds during this time, a decorative feature heavily popularized in New Kingdom faience vessels such as the one in Figure 7. Much as in the case of the thick-walled vessels, objects consisting of a coarse body with a white layer (fine, like the quartz) covering the surface were produced which achieved more brilliant coloration when a glaze was applied. During this time, the method of glazing was either the older efflorescence method or the newer cementation method. Solid evidence for glazing by cementation first appears during the Middle Kingdom (Nicholson and Peltenburg 2000). It should be noted that though the faience industry underwent an array of technological advancements during the Middle Kingdom and First Intermediate

Figure 7: Sphinx of Amenhotep III (ca. 1390-1352 BCE) (Metropolitan Museum of Art 2012b).

Period, glazed stone, specifically steatite, persisted in objects like scarabs (see those in Figure 8). Scarabs require fine, sharply delineated inscriptions that were more readily achieved on steatite than on a faience core. The niche for glazed stone may well explain the development of faience bodies harder than those of most previous faience specimens (Nicholson and Peltenburg 2000).

The faience industry in ancient Egypt reached its peak during the New Kingdom (1550 – 1069 BCE). During this period, faience workers developed the open-face mold, which allowed for the production in great numbers of the smaller objects of the Old Kingdom, like beads and amulets as well as rings. It was during the New Kingdom that Egyptian faience artisans expanded the range of colors they could produce. The development of harder faience bodies during the Middle Kingdom extended into the New Kingdom, finding use in the scarabs that had previously been produced exclusively from glazed steatite. Polychrome tiles and inlays became common during this period and are considered a testament to the skill of the craftsmen of the day. Beyond these tiles and

Figure 8: *Top: left:* Steatite Protection Scaraboid with Hippo. Back (ca. 664-332 BCE); Faience scarab, Kind worshipping solar boat (no date); Steatite Protection Scarab, "Amun is Protection" (ca. 1550-1069 BCE). *Bottom: left:* Faience Royal Name Scarab, "Thutmosis IV" (ca. 1550-1069 BCE); Faience Protection Scarab, Symbols of Rejuvenation, Kingship and Afterlife (ca. 1648-1540 BCE); Faience Royal Named Scarab, "Thutmosis III, King of Upper and Lower Egypt, Lord of the Two Lands" (ca. 1550-1069 BCE) (Tyrrell 2000).

inlays, faience became much more heavily utilized in architecture, as seen in three-dimensional displays like the Amarna grape clusters shown in Figure 9. New Kingdom faience was also heavily exported throughout the Mediterranean and is documented on

both Cyprus and Crete, not to mention mainland Greece (Nicholson and Peltenburg 2000).

Likely a result of the extensive exportation throughout the Mediterranean and Near

Figure 9: Amarna grape clusters (ca. 1353-1336 BCE) (Metropolitan Museum of Art 2012c).

East during the New Kingdom, faience of the Third Intermediate Period (1069 – 664 BCE) became varied and localized to the point that the local copies heavily resembled the Egyptian imports. It is during this period that the technology experienced a decline, including a limitation in color range, a limitation in glass production and an average lowering of the quality of objects produced. A revival beginning during the Twenty-fifth dynasty and extending into the Late Period (664 – 332 BCE), with the Twenty-sixth dynasty, brought new attention to the more traditional art forms throughout Egypt, including faience. High-quality pieces became more desirable, and the range of colors was re-expanded to include new colors, like apple green in addition to older colors, like yellow. It is thought that black glazes were introduced through contact with Greek

mercenaries, though the methods of production for this color differ between Upper and Lower Egypt (Nicholson and Peltenburg 2000).

Compared to previous periods, much less is known regarding faience production in the Ptolemaic (332 – 30 BCE) and Roman (30 BCE – 641 CE) Periods (post-Pharaonic Egypt). Vessels such as bowls and vases from these periods are often distinguished by relief decorations, a feature enhanced by the earlier developed technology of two-tone glazes. Natron becomes much more heavily used as a source of the alkali during these periods, as well as plant ash. After the end of the Roman Period in 641 CE, the technology was adopted and further developed by Islamic faience workers to produce new products stylistically and compositionally distinct from those of the other Egyptian periods (Nicholson and Peltenburg 2000). A summary of faience through the periods of ancient Egypt can be found in Table 1.

Table 1: Temporal Development of Egyptian Faience Technologies.

Period	State of Faience Technology
Predynastic Period 5500 – 3100 BCE	Glazed steatite; Crushed silica core development; small artifacts like beads and amulets; collaboration with goldsmiths; steatite scarabs.
Early Dynastic Period 3100 – 2686 BCE	Small figurines; Predynastic technology.
Old Kingdom 2686 – 2181 BCE	Djoser Step Pyramid; molding; Early Dynastic Period technology.
First Intermediate Period 2181 – 2055 BCE	Little development; Old Kingdom technology without monumental projects.
Middle Kingdom 2055 – 1650 BCE	Thick-walled vessels; decoration of faience; signature blue turquoise color; color variation; First Intermediate Period Technology.
Second Intermediate Period 1650 – 1550 BCE	Darkly painted linear designs; Middle Kingdom Technology.
New Kingdom 1550 – 1069 BCE	Industry peak; open-face mold; faience scarabs; utilization in architecture; Second Intermediate Period technology.
Third Intermediate Period 1069 – 664 BCE	Variation; localization; technological decline; revival.
Late Period 664 – 332 BCE	Revival; reintroduction of color variation.
Ptolemaic Period 332 – 30 BCE	Bowls and vases distinguished by relief decorations; increased use of natron as alkali source.
Roman Period 30 BCE – 641 CE	Bowls and vases distinguished by relief decorations; increased use of natron as alkali source.

Scientific Background

Faience Composition

As described earlier, Egyptian faience is a glazed non-clay-based ceramic composed largely of quartz and a glassy phase (Nicholson and Peltenburg 2000). This glaze is a soda-lime-silicate glass that is often colored by the addition of copper (II) oxide, manganese (II) oxide or a mixture of iron (III) oxide and manganese (IV) oxide. While the composition of faience is somewhat variable, samples typically are composed of 92-99 weight percent silica, 1-5 weight percent calcium oxide and 0.5-3 weight percent sodium oxide (Vandiver and Kingery 1986). Though the objects are made mostly of silica in quartz form, it should be noted that no samples contain silica in the cristobalite polymorphic form (Kiefer and Allibert 1971). In addition, samples of Egyptian faience may contain minor amounts of copper (II) oxide, aluminum oxide, titanium (IV) oxide, magnesium oxide or potassium oxide (Vandiver and Kingery 1986).

Though the primary component of faience is silica, crushed cores of dry silica are unable to maintain their shape. The silica body is combined with water and natron, with or without supplemental lime, a substance found in dry riverbeds, so that it may be shaped (Clark and Gibbs 1997). Since natron was used in the Egyptian embalming process as well as in faience production, several samples have been preserved. Among these samples are bits of natron involved in the embalming of King Tutankhamen (Noble 1969). The chemical composition of the natron described by Noble can be seen in Table 2.

Table 2: Composition of Natron from Tutankhamen Embalming Material (Noble 1969).

Substance	Weight Percent
NaCl	30.6
Na_2SO_4	20.6
SiO_2	10.0
$NaHCO_3$	12.6
Na_2CO_3	4.9
$CaCO_3$	2.0
$MgCO_3$	1.9
Al_2O_3	0.7
Fe_2O_3	0.3
H_2O	4.7
Organic Material	11.7

Egyptian faience may be classified into three categories: standard faience, semi-glass faience and glazed steatite. Standard faience can be identified by its coarse body, while semi-glass faience is set apart by its glassy body. Glazed steatite is an earlier method of producing something akin to faience. It was employed principally for the production of scarabs. Steatite is comprised primarily of talc; its hardness is near one on the Mohs Hardness Scale, thus it is a soft stone that can be carved easily. Once glazed, its hardness increases from one to between three and five (Noble 1969).

Compositionally, each type of faience is unique. The compositions for each type of faience can be seen in Table 3. In the case of standard faience and in the case of the glazed steatite, the glaze appears to form at 950°C based on reproductive experiments (Noble 1969).

Table 3: Faience Compositions (Noble 1969).

Component	Mass in Standard Faience [g]	Mass in Semi-Glass Faience [g]	Mass in Semi-Glass Glaze [g]	Mass in Steatite Glaze [g]
Feldspar ($KAlSi_3O_8 - NaAlSi_3O_8 - CaAl_2Si_2O_8$)	40	0	0	35
Flint (SiO_2)	20	20	0	35
Fine white sand (SiO_2)	8	8	0	0
Na_2CO_3	6	3	35	40
$NaHCO_3$	6	3	0	40
Whiting ($CaCO_3$)	5	0	0	0
Bentonite (clay) (Al_2O_3-$4SiO_2$-H_2O)	2	2	0	0
Copper (II) oxide (CuO)	3	1.5	7	10
Kaolin (clay) (Al_2O_3-$2SiO_2$-$2H_2O$)	0	0	4	14
Dextine (a modified starch)	0	0	18	26
Soda Ash (Na_2O)	0	0	35	0

One of the most comprehensive studies on the composition of faience was carried out by A. Kaczmarczyk and R.E.M. Hedges (1983). In their study, Kaczmarczyk and Hedges (1983) present data separated by element and organized by time period and dynasty. For the study of Third Dynasty Blue-Green faience, the data to consider most heavily include: Green Faience, Dynasties 1-2; Green Faience, Dynasties 3-6; Blue

Faience, Dynasties 1-2; and Blue Faience, Dynasties 3-6. These data sets for the compositions of green and blue faience can be seen in Tables 4 and 5, respectively.

Table 4: XRF-Determined Compositions of Green Faience in Mole Percent (Kaczmarczyk and Hedges 1983).

Compound	Dynasty 1-2		Dynasty 3-6	
	Median	Average	Median	Average
K_2O	0.46	0.82	0.25	0.4
CaO	1.98	3.03	1.39	1.94
TiO_2	0.04	0.06	0.01	0.03
V_2O_5	0.00	0.03	0.00	0.01
MnO_2	0.02	0.06	0.01	0.06
Fe_2O_3	0.26	0.32	0.25	0.75
CoO	0.00	0.01	0.00	0.01
CuO	2.33	2.87	2.41	2.62
ZnO	0.02	0.10	0.01	0.07
SrO	0.00	0.00	0.00	0.00
SnO	0.00	0.01	0.00	0.01
SbO	0.00	0.01	0.01	0.01
BaO	0.00	0.01	0.00	0.04
PbO	0.00	0.00	0.00	0.03
SiO_2	89.6	88.3	90.7	90.2
Cl^-	0.24	0.31	0.00	0.14
SO_3	0.23	0.31	0.00	0.11

Table 5: XRF-Determined Compositions of Blue Faience in Mole Percent (Kaczmarczyk and Hedges 1983).

Compound	Dynasty 1-2		Dynasty 3-6	
	Median	Average	Median	Average
K_2O	1.34	1.43	0.80	1.28
CaO	5.46	7.22	2.79	5.28
TiO_2	0.04	0.06	0.01	0.02
V_2O_5	0.00	0.00	0.00	0.01
MnO_2	0.02	0.11	0.02	0.08
Fe_2O_3	0.48	0.51	0.60	0.61
CoO	0.00	0.00	0.00	0.00
CuO	2.39	3.81	6.09	6.20
ZnO	0.00	0.01	0.00	0.01
SrO	0.02	0.02	0.00	0.03
SnO	0.01	0.09	0.00	0.01
SbO	0.00	0.00	0.00	0.01
BaO	0.00	0.01	0.00	0.01
PbO	0.00	0.00	0.00	0.03
SiO_2	83.8	82.8	85.2	82.7
Cl^-	0.17	0.23	0.04	0.23
SO_3	0.12	0.21	0.07	0.12

Methods of Glazing

Egyptian faience is not typically categorized by composition, but it can be categorized by the method of glazing, of which there are three. The first method is known as application glazing; it involves applying the glaze in a powder or liquid form to the core of the object before firing. This glaze is formed either directly from the raw materials as a fine powder or by combining that powder with water. This powder or slurry can then be applied to the core of the object in a variety of ways, including pouring and dipping (Tite and Bimson 1986).

The second method is referred to as efflorescence glazing. This method differs from application glazing in that the glaze develops from the body of the object instead of from a powder or slurry applied to the body. Water-soluble salts incorporated within the faience body are deposited on the surface of the object (or effloresced) as the object dries. This effloresced layer of salts is what becomes the glaze during firing (Tite and Bimson 1986).

The final method is known as cementation glazing and is somewhat similar to application glazing. In this method of glazing, the body of the object is surrounded by powder instead of being brushed or dipped in a powder or slurry. This body and powder combination is then heated, and the glaze is formed as a result of the chemical reaction at the interface between the body and the portion of the powder in contact with the body (Tite and Bimson 1986).

When studying the microstructure of faience samples, there are four criteria by which the method of glazing may be discerned. One aspect of the microstructure to consider is the glaze layer's thickness. Immediately under the glaze layer is what is

known as the glaze-core interaction layer; its thickness is the second criterion to consider. In addition to measuring the thicknesses of layers, considering the boundary between the body's quartz core and the surface glaze layers is the third aspect of the microstructure. The fourth and final aspect of the microstructure to consider relates to the glassy phase within the core, specifically the extent to which it is present (Tite and Bimson 1986; Tite 1987).

When examining the microstructure, the direct application glazing method may appear in two forms, defined as: ground (fired) frit glazing mixture and raw (unfired) glazing mixture. Direct application of a ground frit glazing mixture is characterized by thick surface glazes and glaze-core interaction layers. In contrast, direct application of a raw glazing mixture is characterized by the absence of the surface layer of glaze and a widely variable glaze-core interaction layer. For ground frit glazing mixtures, the boundary layer is clearly defined, but it is much less well defined for raw glazing mixtures, since the glaze-core interaction layer appears to mix into the quartz core of the object. In terms of the amorphous phase within the core, none is present in the case of ground frit glazing mixtures. The same is true for raw glazing mixtures at locations far from the boundary, but near the boundary there is enough glass in the core for bonding between adjacent quartz crystal apices to occur (Tite and Bimson 1986). These distinctions can be observed in Figures 10 and 11.

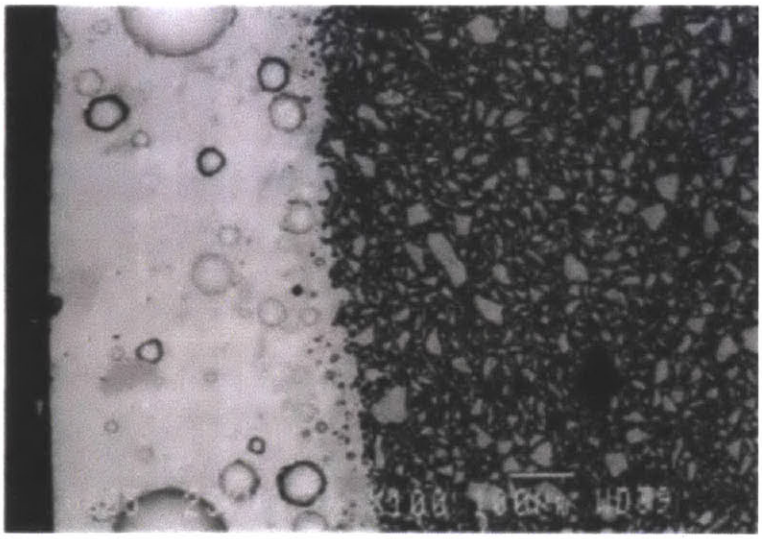

Figure 10: Microstructure of Application Glazing (fired) (Tite and Bimson 1986).

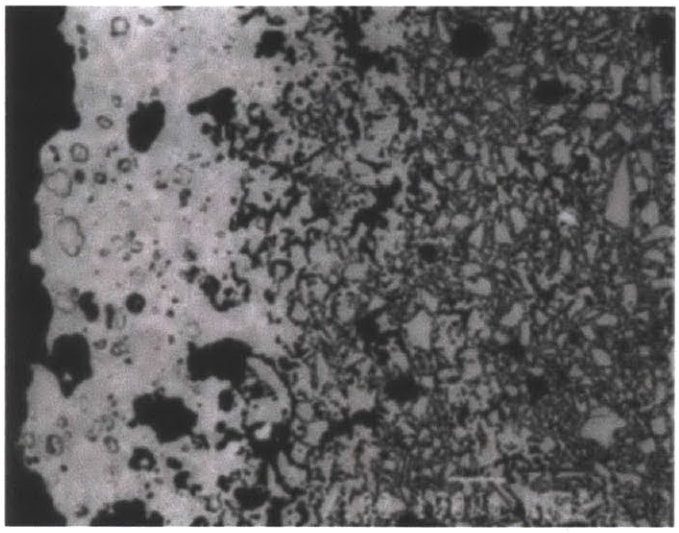

Figure 11: Microstructure of Application Glazing (raw) (Tite and Bimson 1986).

Efflorescent glazes tend to have thick surface glazes and glaze-core interaction layers, much like the direct application of ground frit glazing mixtures. Like the direct application of raw glazing mixtures, though, efflorescent glazes tend to have ill-defined boundary layers, which makes it difficult to distinguish the cores from the glaze-core interaction layers.

A defining characteristic of any type of direct application glaze method is the presence of glass in the core. Though some glass exists in the direct application of raw glazing mixtures near the glaze boundary, the glass is extensive for efflorescent glazes (Tite and Bimson 1986). An example of this microstructure can be observed in Figure 12.

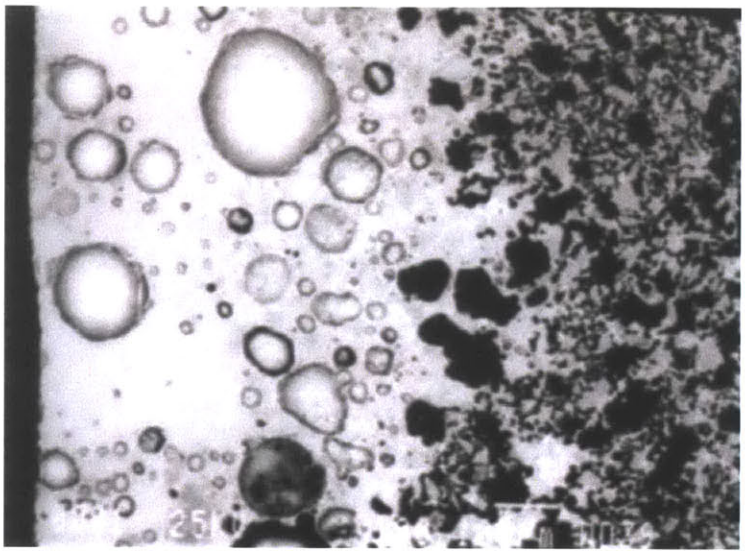

Figure 12: Microstructure of Efflorescence Glazing (Tite and Bimson 1986).

Cementation glazes possess thin, irregular surface glaze layers and thicker glaze-core interaction layers. In these regards, they bear some resemblance to cases of direct application of a raw glazing mixture. A distinguishing characteristic, then, of cementation glazes is the clearly defined boundary between the glaze-core interaction layer and the object's quartz core. Objects with cementation glazes also exhibit quantities of an amorphous phase near the boundary sufficient to cause bonding between adjacent quartz crystal apices (Tite and Bimson 1986). An example of this microstructure can be observed in Figure 13.

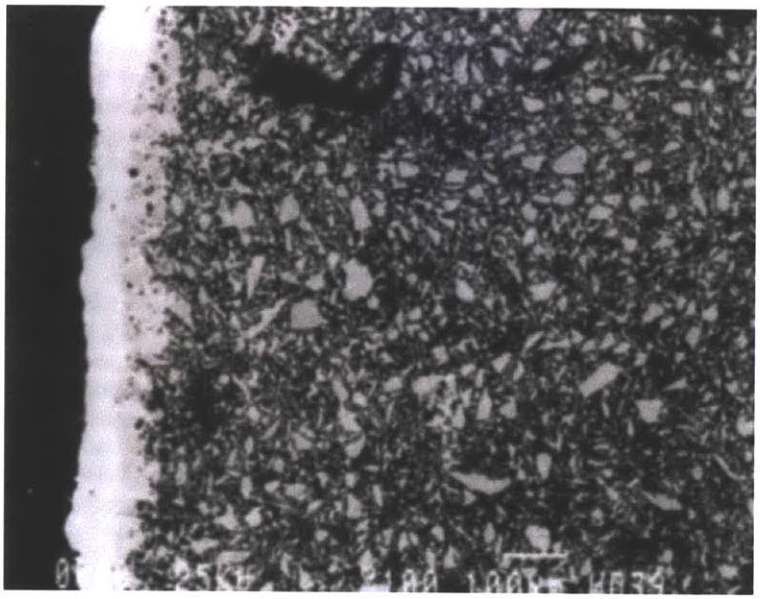

Figure 13: Microstructure of Cementation Glazing (Tite and Bimson 1986).

Firing Faience

Samples with glazes formed by direct application glazing do not exhibit changes in the microstructure described when heated from 850°C to 900°C. The same is true for those samples with glazes formed by efflorescence glazing. Glazes produced by the method of cementation glazing, however, do not form below 850°C, thus samples produced using that method of glazing would need to be fired at higher temperatures (Tite and Bimson 1986). As mentioned previously, faience samples do not contain cristobalite, a polymorphic form of silica that forms at 920°C (Kiefer and Allibert 1971). Noble (1969) notes similar firing ranges from experiments to create Egyptian faience based on the compositional data reported in Tables 2 and 3. Based on experimental reproduction, the consensus has been that Egyptian faience must have been heated to temperatures in the range of 850°C to 950°C in order for glaze formation to occur.

Possible Low Temperature Glaze Formation

The approximately 36,000 faience tiles of Djoser's Step Pyramid have been assumed to have been glazed using either the method of direct application (by dipping) or by the method of efflorescence (Kiefer and Allibert 1971; Schiegel 1988). As such, the firing range has been determined to be between 800°C and 850°C based on reproductive experiments. Davidovits and Davidovits (2004) determined the presence of phosphorus in a Djoser tile that they analyzed by scanning electron microscopy (SEM). This led them to suggest that turquoise may have been used as a component of tiles glazed by efflorescence in the production of the tile. Their subsequent attempts to replicate the Djoser tiles using a synthetic turquoise mixture as a source of phosphorus resulted in the stable, turquoise-colored, efflorescence-glazed tiles that appear identical to the Egyptian faience tiles (Davidovits and Davidovits 2004). They produced these replicas at temperatures as low as 250°C to 350°C. Heating above 350°C turned the tiles from a turquoise-blue to a grey or black color. It has also been noted that though blue was considered the most prestigious color to the ancient Egyptians, the color of the tiles found in the Djoser Step Pyramid vary, including green, grey and black as well as blue (Davidovits and Davidovits 2004).

Formulation of the Research Problem

If the glaze of Djoser Step Pyramid faience tiles formed in the range of temperatures between 250°C and 350°C, as suggested by Davidovits and Davidovits (2004), instead of at the higher, ranges of 850°C to 950°C previously suggested for most Egyptian faience, the Egyptian faience from the Djoser Step Pyramid should have a composition that allows low temperature glazing to occur. The research reported in this thesis attempts to address this issue: what in the composition of the Djoser Step Pyramid faience tiles could facilitate such a low temperature glaze?

Materials and Methods

Djoser Faience Tile

In order to answer the questions posed concerning the composition of these Old Kingdom faience tiles, a faience tile from the Djoser Step Pyramid (2667-2648 BCE) was provided for analysis by Prof. Joseph Davidovits of the Geopolymer Institute who has the artifact on loan from a private collector. The tile studied is shown below in Figure 14. The tile measures 5.5 cm in length, 4.3 cm in width and 1.2 cm in depth. The tile is thickest near the center; closer to the edges the depth falls to 0.7 cm. The tile weights 27.23 g. In the field of archaeology, all artifacts are considered unique. Some are irreplaceable. Because of this issue, especially in the case of intact (i.e., unbroken) artifacts, a variety of non-destructive analytical methods has been developed to study these artifacts in the laboratory. The Djoser faience tile was analyzed using these methods.

Figure 14: A faience tile from the Djoser Step Pyramid.

X-Ray Fluorescence

X-Ray Fluorescence (XRF) is a method by which a sample is irradiated with x-rays so that the constituent elements radiate fluorescent x-rays. The measured energies of these fluorescent x-rays can be used to determine the elemental composition of the irradiated sample.

The XRF data collection reported here was carried out using a Bruker Tracer III-SD Handheld X-Ray Fluorescence Spectrometer in the X-Ray Diffraction Shared Experimental Facility of the MIT Center for Materials Science and Engineering (CMSE). The device was oriented such that the sample stage and cover were placed on top and were level in the horizontal as depicted in Figure 15. The x-ray beam is emitted from the opening at the arrow (Figure 15), and the fluoresced x-rays are measured in the opening

The Sample Table

The Sample Shield

Figure 15: XRF Experimental Setup (Speakman 2011).

opposite the point of emission. The device uses a rhodium source for the x-rays as well as a set of palladium slits. Using this device, detectable elements are those between and including magnesium and plutonium.

The device features a variety of settings for specific analyses. In addition to the General Elemental Analysis, the following analyses were performed: Analysis of Light Elements (copper and below, except sulfur and chlorine); Analysis of Light Elements (iron and below, except titanium and scandium); and Analysis of Higher Atomic Number Elements (iron to molybdenum) for ceramics. The settings for each method are detailed in Table 6.

Table 6: Methods of XRF Analysis Employed (Speakman 2011).

Method	Voltage	Current	Filter	Vacuum
General Elemental	40 kV	15 μA	None	On
Light Elements (below Cu)	15 kV	55 μA	None	On
Light Elements (below Fe)	15 kV	55 μA	Blue	On
Higher Atomic Number	40 kV	15 μA	Green	Off

In order to gain a more complete understanding of the composition of the Djoser faience tile, measurements were taken in five orientations: on the top, glazed surface of the tile along its long dimension (Top Long, Figure 16), on the top, glazed surface of the

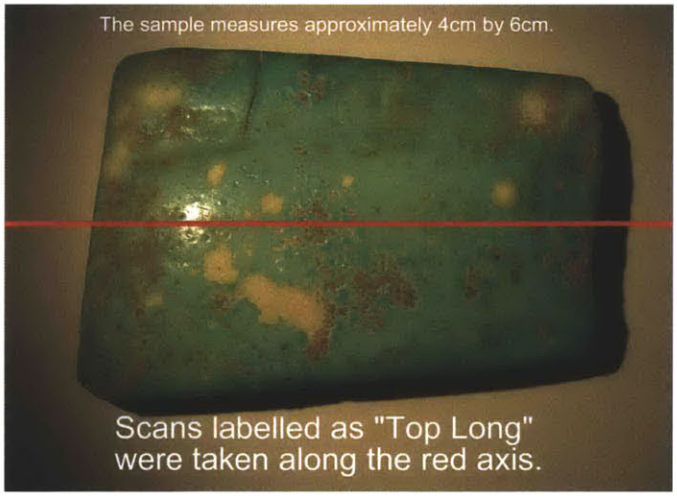

Figure 16: The Top Long Orientation.

tile along its short dimension (Top Short, Figure 17), on the bottom surface of the tile along its long dimension (Bottom Long, Figure 18), on the bottom surface of the tile along its short dimension (Bottom Short, Figure 19) and along the long dimension of the broken side (Side White, Figure 20).

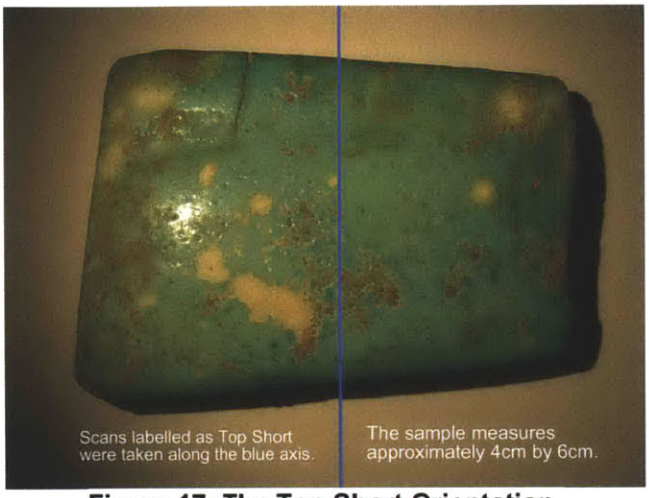

Figure 17: The Top Short Orientation.

Figure 18: The Bottom Long Orientation.

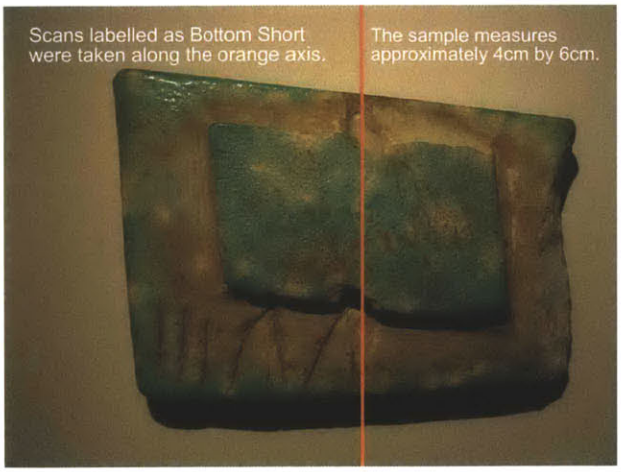

Figure 19: The Bottom Short Orientation.

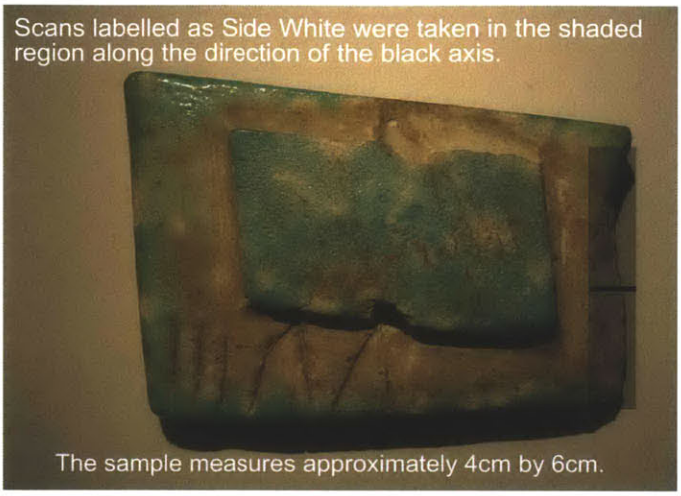

Figure 20: The Side White Orientation.

Environmental Scanning Electron Microscopy

Environmental Scanning Electron Microscopy (ESEM) is a method by which an artifact or a sample, placed in a vacuum chamber, is bombarded with a beam of electrons. The electron particles' interactions with the material result in data used to produce high-magnification images and to reveal information about the sample's composition and topography. Samples for ESEM data collection do not require preparation, which makes it preferable to Scanning Electron Microscopy (SEM) for use in archaeological studies.

The ESEM data collection was carried out using a FEI/Philips XL30 FEG Environmental Scanning Electron Microscope in the Electron Microscopy Shared Experimental Facilities of the MIT CMSE. The Djoser faience tile was small enough to fit inside the chamber. It was analyzed in two orientations: on the top, glazed surface and along the broken edge near the glaze-core boundary. These orientations allowed for analysis of the surface glaze (Top Near Center, similar to Figures 16 and 17) and of the internal core (Side White, similar to Figure 20).

X-Ray Energy Dispersive Spectroscopy

X-Ray Energy Dispersive Spectroscopy (XEDS) is a method used here in conjunction with ESEM. As the electrons interact with the sample, x-rays are produced that are separated by energy into spectra generated by the elements within the sample. Through the method of XEDS, the measured x-ray spectra can be used to generate the elemental compositions of the sample.

Unlike the XRF elemental analysis, this method of XEDS allows for the detection of much lighter elements such as sodium and oxygen. Thus the elemental composition

analyses may differ between the two methods depending on the composition of the sample. Since the device for XEDS determination is an attachment to the ESEM equipment, the data collection was performed simultaneously using the same orientations described for the ESEM methods. This allowed for comparison of compositions of both the glaze and the core of the Djoser faience tile.

X-Ray Diffraction

X-Ray Diffraction (XRD) is a method by which a sample is irradiated with x-rays so that the constituent crystals diffract the incident beam. The measured angles of diffraction produce a spectrum to be compared to standard spectra of known compounds in order to determine the compounds present in the sample. XRD is also used to determine the crystalline structure and degree of crystallinity of the irradiated material..

The XRD data collection was carried out using a PANalytical X'Pert Pro MPD using the Open Eularian Cradle configuration in the X-Ray Diffraction Shared Experimental Facility of the MIT CMSE. The sample was analyzed in three orientations: the large glazed surface on top (Top Blue, similar to Figures 16 and 17), the broken surface on top (Side White, similar to Figure 20) and the underside of the tile on top (Bottom Near VVIII, similar to Figures 18 and 19). The VVIII designation refers to a series of hatchings on the bottom side of the Djoser faience tile. These different orientations allowed for comparisons of the crystal structure of various areas on the tile, particularly how the glazed structure compares to the structure without the glaze.

X-Ray Micro-Computed Tomography

X-Ray Micro-Computed Tomography (micro-CT) is a method by which an object is irradiated with x-rays so as to generate cross-sections of the object that later can be used to recreate a three-dimensional, virtual model of the object. This model can then be used to generate two-dimensional images from a variety of perspectives within and around the object.

The micro-CT data collection was carried out using an XT H 160 Nikon Metrology micro-CT scanner in the MIT Center for Bits and Atoms (CBA). The Djoser faience tile was analyzed in a polymer casing, and a three-dimensional image of the tile was generated. This is an entirely non-destructive analytical instrument for scanning small objects.

Analytical Results

X-Ray Fluorescence

The general elemental analysis oriented along all five directions indicated the presence of aluminum, silicon, phosphorus, potassium, calcium, titanium, manganese, iron, nickel, copper, zinc and strontium. Rhodium and palladium peaks are also observed due to the source and slits of the device, respectively. The presence of these peaks potentially masks the peaks for sulfur and chlorine.

The analysis of light elements (copper and below, except sulfur and chlorine) oriented along all five directions indicated the presence of silicon, phosphorus, potassium, calcium, titanium, manganese, iron and copper. Rhodium and palladium peaks are, again, observed, possibly masking sulfur and chlorine.

The analysis of light elements (iron and below, except titanium and scandium) oriented along all five directions indicated the presence of aluminum, silicon, phosphorus, sulfur, chlorine, potassium, calcium, manganese and iron. The use of the blue filter for this scan removes the rhodium and palladium peaks, revealing the previously hidden sulfur and chlorine peaks. Because the titanium in the blue filter absorbs much of the radiation from the rhodium source and palladium plates, the titanium peak does not reflect only the titanium in the Djoser faience tile.

The analysis of higher atomic number elements (iron to molybdenum) for ceramics oriented along all five directions indicated the presence of iron, copper, zinc and strontium. This method of analysis does not detect the lighter elements, but it is optimized for those elements between rubidium and niobium inclusive, which includes strontium.

Using the results from the specialized analyses, it was possible to determine those elements that were not revealed in the General Elemental Analysis. When measured relative to a reference element (such as iron, copper or silicon), the ratios determined by XRF analysis most closely resemble relative atomic percentages. The elements detected in the tile have been normalized to iron, copper and silicon for each of the five orientations shown in Figures 16 to 20. These results are reported in Table 7. Since silica is the primary component of the glaze and body, Table 7 provides the greatest insight into the composition of the material.

In general, the largest elements detected were copper (the coloring agent), silicon (the primary constituent of the glaze and the core) and iron. Calcium is present in a high ratio to silicon in the surface glaze (nearly a one-to-one ratio). In fact, many of the same elements described by Kaczmarczyk and Hedges (1983) appear in this XRF analysis. Notably present is phosphorus, not described in the study by Kaczmarczyk and Hedges (1983); the ratio of phosphorus to silicon ranges from approximately 0.1 to 1.6%. Using the results obtained from XRF analysis, it is possible to consider the likelihoods of proposed compositions for the Djoser faience tile.

Table 7: Silicon-Normalized XRF Analyses, Expressed as Relative Atomic Fractions.

Element	Top Long	Top Short	Bottom Long	Bottom Short	Side White
Al	0	0	0	0	0
Si	1	1	1	1	1
P	0.001	0.002	0.004	0.003	0.016
S	0.026	0.030	0.014	0.012	0.141
Cl	0.137	0.139	0.097	0.074	0.461
K	0.026	0.030	0.017	0.015	0.017
Ca	0.935	1.085	0.262	0.187	0.494
Ti	0.016	0.017	0.016	0.016	0.117
Mn	0.027	0.029	0.022	0.019	0.126
Fe	0.496	0.523	0.387	0.297	1.102
Ni	0.048	0.050	0.037	0.032	0.299
Cu	7.020	6.683	3.682	3.001	1.256
Zn	0.118	0.120	0.065	0.0517	0.056
Sr	0.092	0.103	0.042	0.0284	0.099

Environmental Scanning Electron Microscopy

Directly, the ESEM provides images to be examined. Figure 21 depicts an area of the glazed surface of the Djoser faience tile taken near the tile center where it is green in color, while Figure 22 depicts an area near the boundary of the broken white edge and the

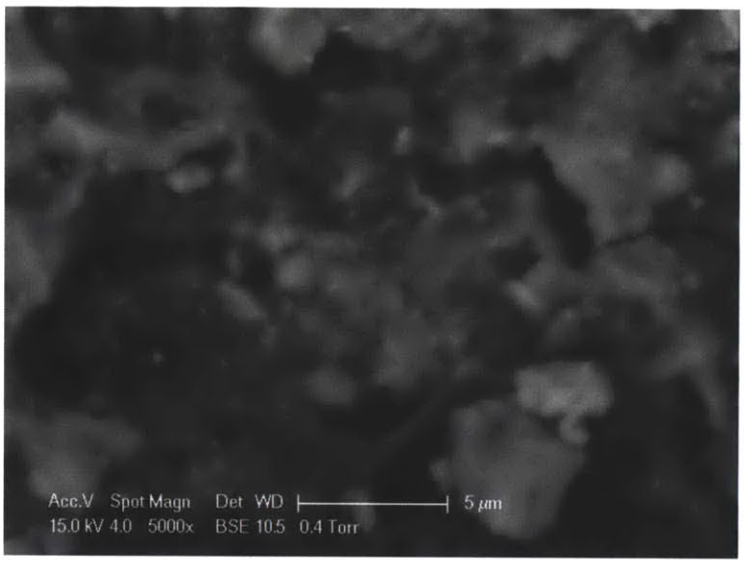

Figure 21: ESEM Image from Top Near Center Orientation.

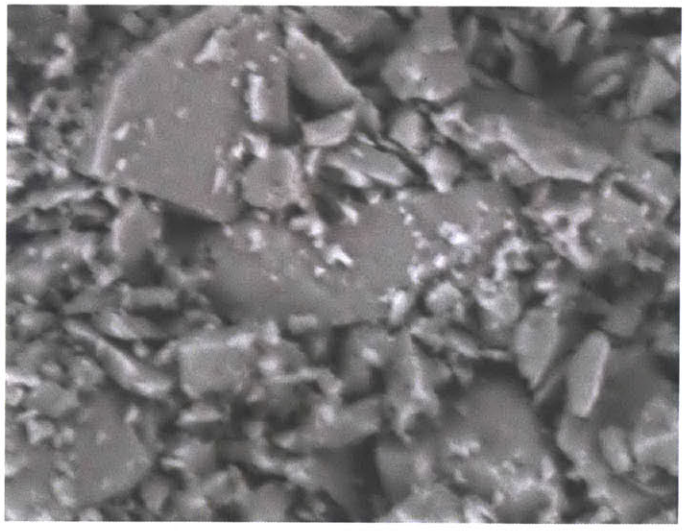

Figure 22: ESEM Image from Broken White Edge Orientation. Same scale as Figure 21.

glazed surface of the tile. Both images are at a magnification of 5,000, with a scale bar of 5 μm. Each image is representative of the surface from which it is taken. The glazed surface depicted in Figure 21 exhibits a more continuous microstructure. In comparison, the core surface depicted in Figure 22 is characterized by a greater fraction of crystalline material with much less evidence of a glassy network between the crystals.

X-Ray Energy Dispersive Spectroscopy

Using the ESEM in conjunction with the XEDS analytical feature, two forms of related data were obtained. The XEDS methods produced dot maps that indicate the locations and relative abundances of elements on the surface captured by ESEM. These dot maps were then overlain on the ESEM images in order to determine the composition of various surface features at distinct locations (see Figures 23-27).

For the Top Near Center orientation, Figures 23, 24 and 25 display dot map overlays for sodium and chlorine, calcium and carbon and silicon and phosphorus, respectively. The correlation in the overlay of Figure 23 suggests the presence of sodium chloride crystals within the sample; sodium is represented by yellow dots, and chlorine is represented by green dots. The correlation in the overlay of Figure 24 may

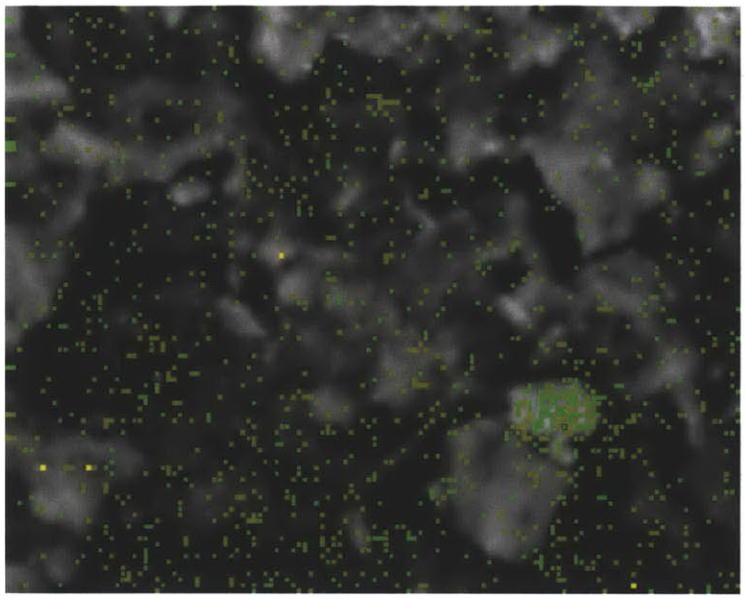

Figure 23: Sodium (yellow) and Chlorine (green) Overlay for Top Near Center Orientation.

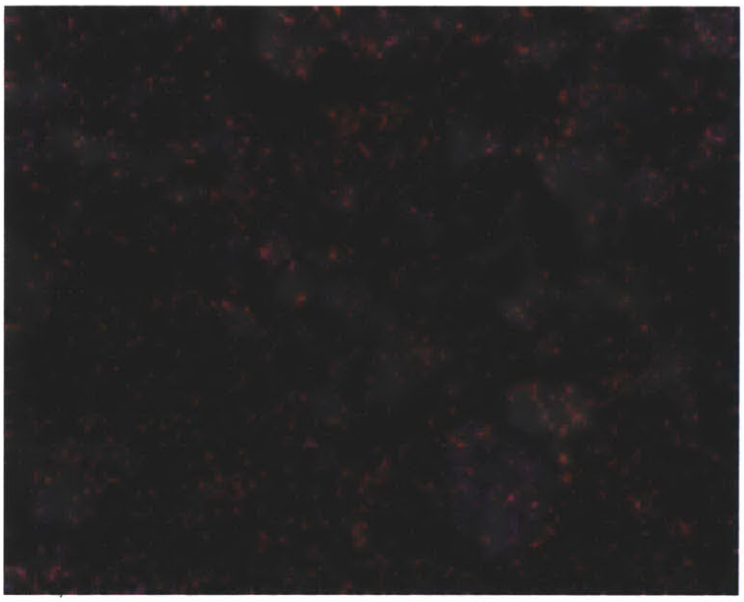

Figure 24: Carbon (red) and Calcium (violet) Overlay for Top Near Center Orientation. Note that carbon is near the edge of elemental detectability for XEDS.

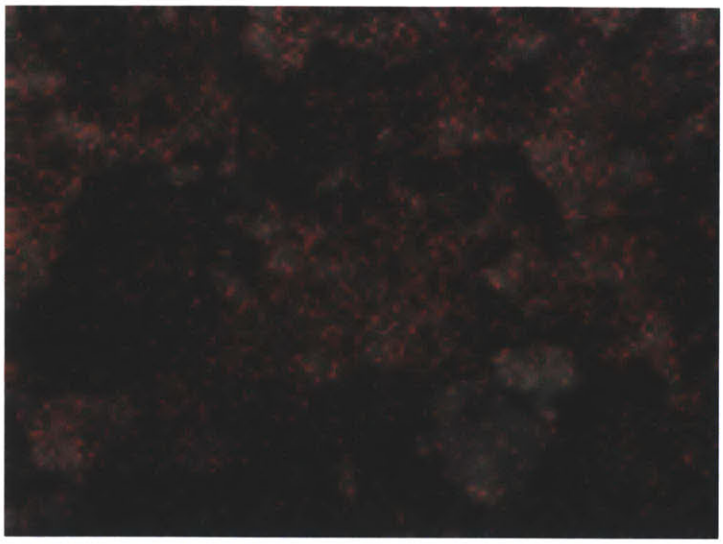

Figure 25: Silicon (red) and Phosphorus (green) Overlay for Top Near Center.

suggest that the calcium compound is present as calcium carbonate rather than as calcium oxide; calcium is represented by violet dots, and carbon is represented by red dots. The overlay in Figure 25 demonstrates the amount of silicon present in the surface as well as the distribution of phosphorus throughout the silica; silicon is represented by red dots, and phosphorus is represented by green dots. Though phosphorus is detectable in the glaze surface, it appears to occur in quite low quantities compared with silicon.

For the Side White orientation, dot map overlays are shown for calcium and carbon in Figure 26 and for silicon and phosphorus in Figure 27. The correlation between calcium and carbon in Figure 26 (calcium is represented by red dots, and carbon is represented by green dots) might be used along with the overlay of carbon and calcium in Figure 24 as a way to determine the form in which calcium is present in the sample. In the area captured in Figure 26, the signal is faint, and it is not possible to determine in what form the calcium is present. The correlation between silicon and phosphorus in Figure 27 might be used, along with the information for silicon and phosphorus gathered from Figure 25, to examine the distribution of phosphorus within the silica network;

silicon is represented by yellow dots, and phosphorus is represented by pink dots. Here, however, the signal from the phosphorus is too faint to make a determination regarding a relationship between the two elements.

In addition to the dot maps, XEDS allows for the computation of elemental compositions based on the analyses provided by the dot maps. When measured relative to

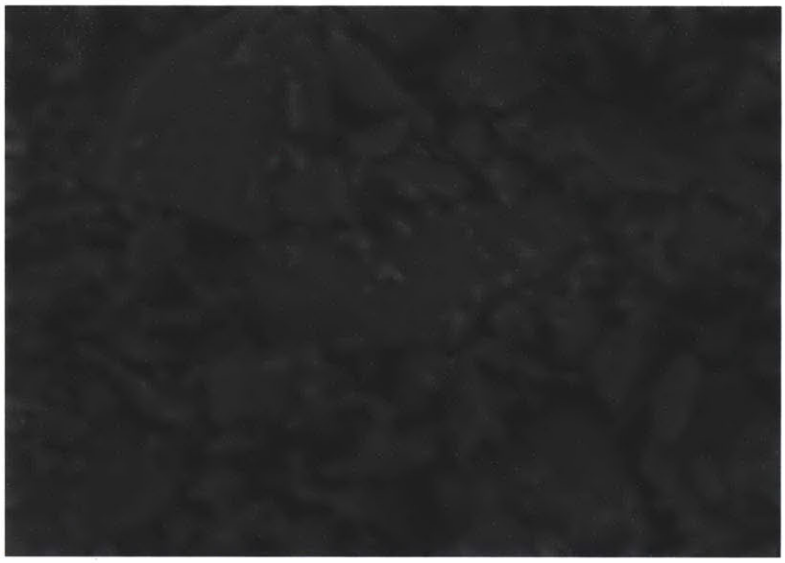

Figure 26: Calcium (red) and Carbon (green) Overlay for Side White Orientation.

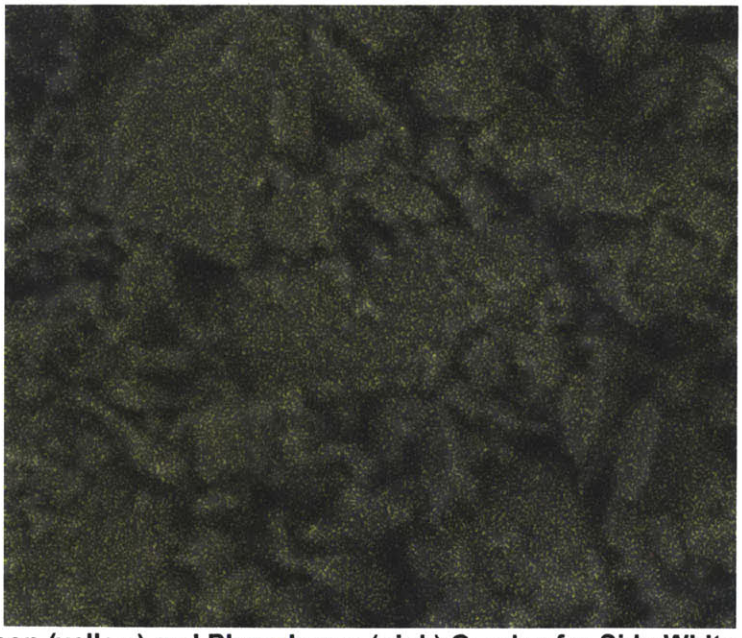

Figure 27: Silicon (yellow) and Phosphorus (pink) Overlay for Side White Orientation.

a reference element, as in the case of XRF, the data obtained reflect most closely the relative atomic percentages of elements within the sample. While these percentages can be compared to those obtained by XRF, it should be noted that XEDS analyses detect the presence and measure the relative abundance of elements lighter than magnesium, a feature that XRF lacks.

In the case of the Top Near Center orientation, XEDS was able to detect carbon, oxygen, sodium, magnesium, copper, aluminum, silicon, phosphorus, sulfur, chlorine, calcium and iron. The XEDS spectrum for the Top Near Center orientation is presented in Figure 28. Given the high levels of carbon and oxygen present, it is useful to generate a set of compositions that omit both of those elements. Though sodium and magnesium are present in the XEDS analyses, normalizing the data to a reference element allows for more accurate comparison with the data obtained through XRF analyses.

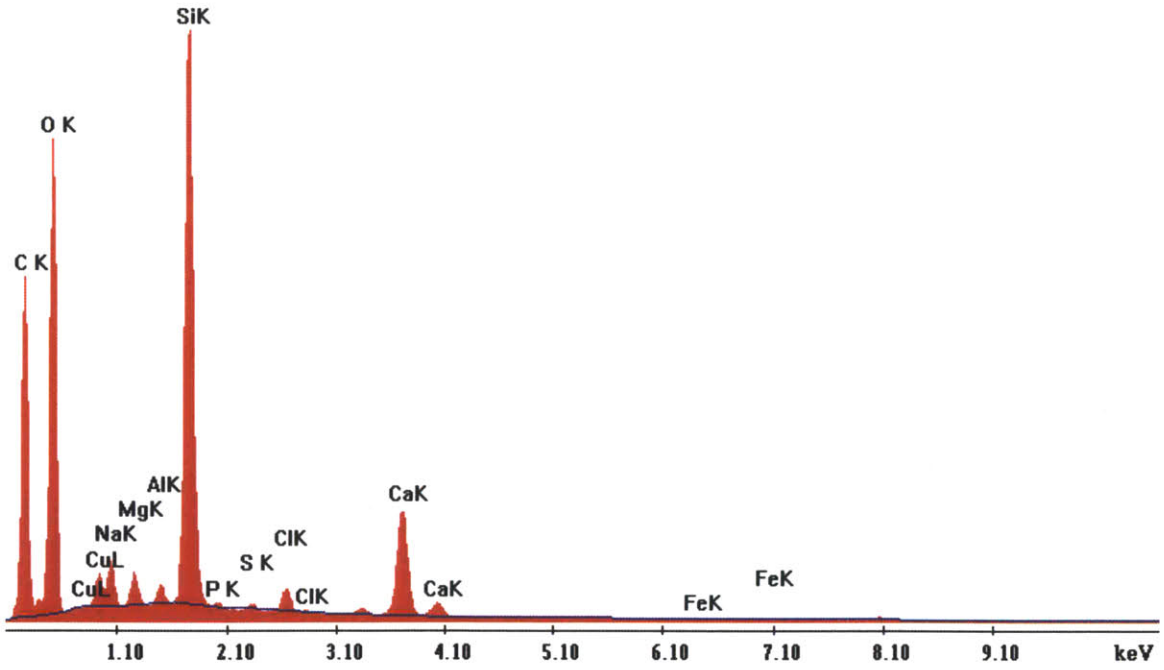

Figure 28: XEDS Spectrum for the Top Near Center orientation.

In the case of the Side White orientation, XEDS was able to detect carbon, oxygen, copper, aluminum, silicon and calcium. The XEDS spectrum for the Side White orientation is presented in Figure 29. Again, it is useful to remove carbon and oxygen from the composition to be considered, to compute detectable cation atomic percents for the glaze and the core (Tables 8 and 9, respectively) and to normalize these remaining cationic elements for comparisons with data obtained from XRF analyses.

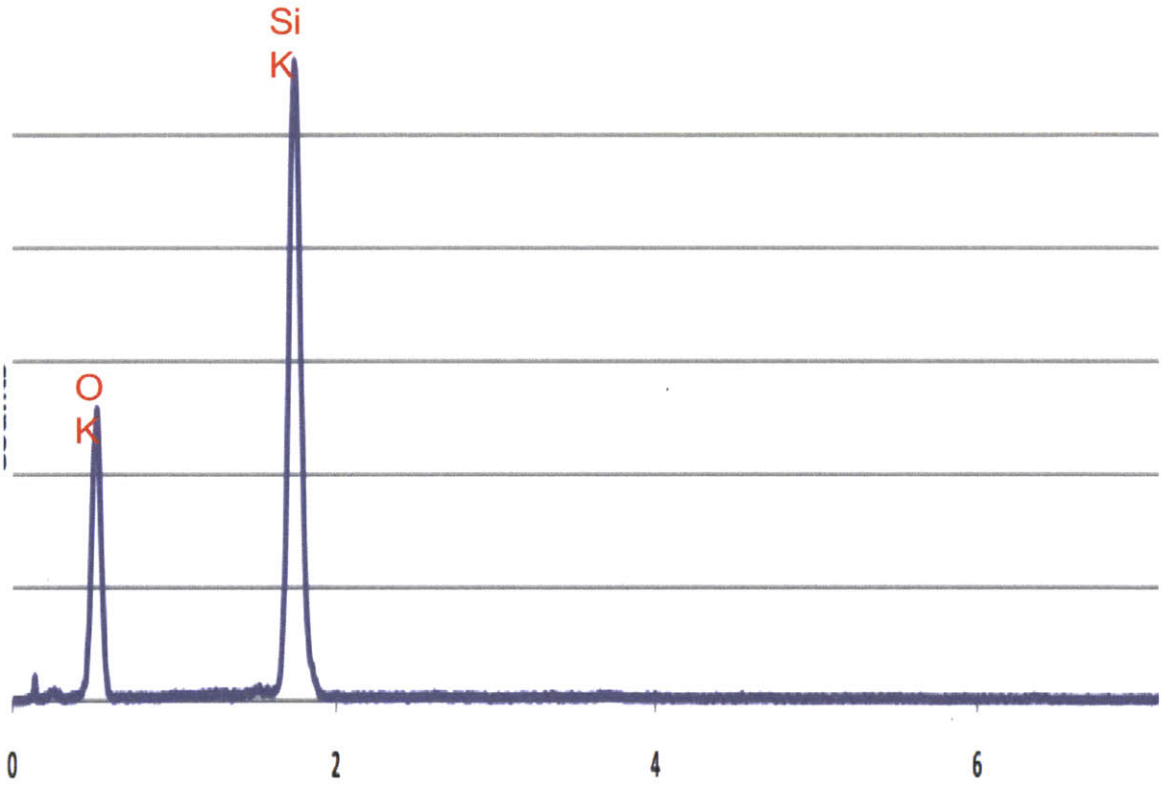

Figure 29: XEDS Spectrum for the Side White orientation.

Table 8: Cation percentages from XEDS for the Djoser faience tile blue glaze.

Element	*Wt%*	*At%*
Cu	6.00	2.99
Na	4.21	5.78
Mg	2.89	3.75
Al	1.62	1.89
Si	53.5	60.2
P	0.51	0.53
S	0.87	0.86
Cl	3.74	3.33
Ca	25.0	19.7
Fe	1.75	0.99

Table 9: Cation percentages from XEDS for the Djoser faience tile core.

Element	*Wt%*	*At%*
Cu	0	0
Al	0.62	0.65
Si	98.7	98.9
P	0	0
S	0	0
Ca	0.70	1.05
Fe	0	0

The elemental analysis (without carbon and oxygen) measured relative to silicon is presented in Table 10. It should be noted that the only elements detected in the Side White orientation after removing carbon and oxygen were aluminum, silicon and calcium. According to the results in Table 10, the ratio of phosphorus to silicon is approximately 0.009 in the glaze compared with 0.0013 obtained through XRF. XEDS has a far shallower depth of penetration than does XRF, and no phosphorus was detected in the body by XEDS. Because XRF penetrates into the core, the values obtained through XRF for the phosphorus-silicon ratio should be lower than the glaze values for the phosphorus-silicon ratio obtained through XEDS. The presence of specific elements (those heavier than magnesium) detected through XEDS analysis is confirmed by the XRF analysis.

Table 10: Silicon-Normalized XEDS Analyses, Expressed as Relative Atomic Percents.

Element	Top Near Center	Side White
Cu	0.05	0
Na	0.10	0
Mg	0.06	0
Al	0.03	0.006
Si	1	1
P	0.01	0
S	0.01	0
Cl	0.06	0
Ca	0.33	0.004
Fe	0.02	0

X-Ray Diffraction

The Top Blue orientation (comparable to Figures 16 and 17) is the one that provides the best insight into the composition of the Djoser faience tile glazes. The XRD analysis for the Top Blue orientation suggests the presence of three crystalline phases. Silicon oxide (grey in Figures 30 and 31) in the form of quartz and calcium carbonate (blue in Figures 30 and 31) are almost certainly present. The low angle peak observed in Figures 30 and 31, however, appears to correspond to silicon phosphate (SiP_2O_7) (green). Similar peaks attributed here to silicon phosphate have previously been attributed to the compound paratacamite ($Cu_2Cl(OH)_3$) (Manti, *et al.* 2008). Paratacamite does not have a wide geographic distribution and is uncommon. Because of this, the silicon phosphate

more likely completes the spectrum than does the paratacamite. Unfortunately, because the silicon phosphate phase does not have a documented reference intensity ratio (RIR), it was not possible to generate a quantitative crystalline phase composition. Notice the hump in Figure 30; this is indicative of a significant glassy phase (the surface glaze).

The XRD analysis in Figures 32 and 33 for the Bottom Near VVIII orientation (comparable to Figures 18 and 19) did not indicate the presence of silicon phosphate, which occurs in the Top Blue analysis. Both quartz (red in Figures 32 and 33) phases and calcium carbonate (blue in Figures 32 and 33) phases were observed again. Since both crystal structures have well-defined RIRs, it was possible to quantify the crystalline composition. Based on the XRD data available, this orientation yields a crystal component composed of 99% silicon oxide and 1% calcium carbon oxide by weight percent. Though a significant amorphous region was visible for the spectrum in Figure 30, there appears to be little to no amorphous component in this orientation. Since there is little glaze on the surface analyzed in Figure 32, it is likely that the amorphous phase is limited to the glaze.

While the Bottom Near VVIII orientation provides more insight into the core of the Djoser faience tile, the best information from the core comes from the Side White orientation (comparable to Figure 20). As with the two previous orientations, phases of quartz (red in Figures 34 and 35) and calcium carbonate (grey in Figures 34 and 35) are likely present. It is in this orientation that a potential phase of calcium sulfate first appears in the spectrum seen in Figures 34 and 35, coded in maroon. Since it does not appear in the other orientations, it may not be present at all; however, including this new phase completes the identification of the major peaks in this spectrum. Since all three

phases have well-defined RIR values, it is possible to determine the mass percent components of the crystalline phases. Based on the Side White Analysis, the crystalline phase is 97% silicon oxide, 2% calcium carbonate and 1% calcium sulfate. In this orientation, a small amorphous region is visible in Figure 34; however, it is much less significant than the region seen in Figure 30. Due to the nature of the XRD analysis, the beam may have penetrated through to the glaze, which would cause the detection of a small amorphous phase. This result is consistent with the observations for the Bottom Near VVIII and Top Blue orientations.

While these are the phases that produce the strongest signals, it is possible that other crystalline phases are also present. It is also possible that some of the phases identified may not be present in the sample. Since the spectra of the tile are most complete with the inclusion of the phases mentioned, however, this is not likely the case. In addition to the crystalline phases, there is a substantial amorphous component to the tile, particularly in the outer glaze.

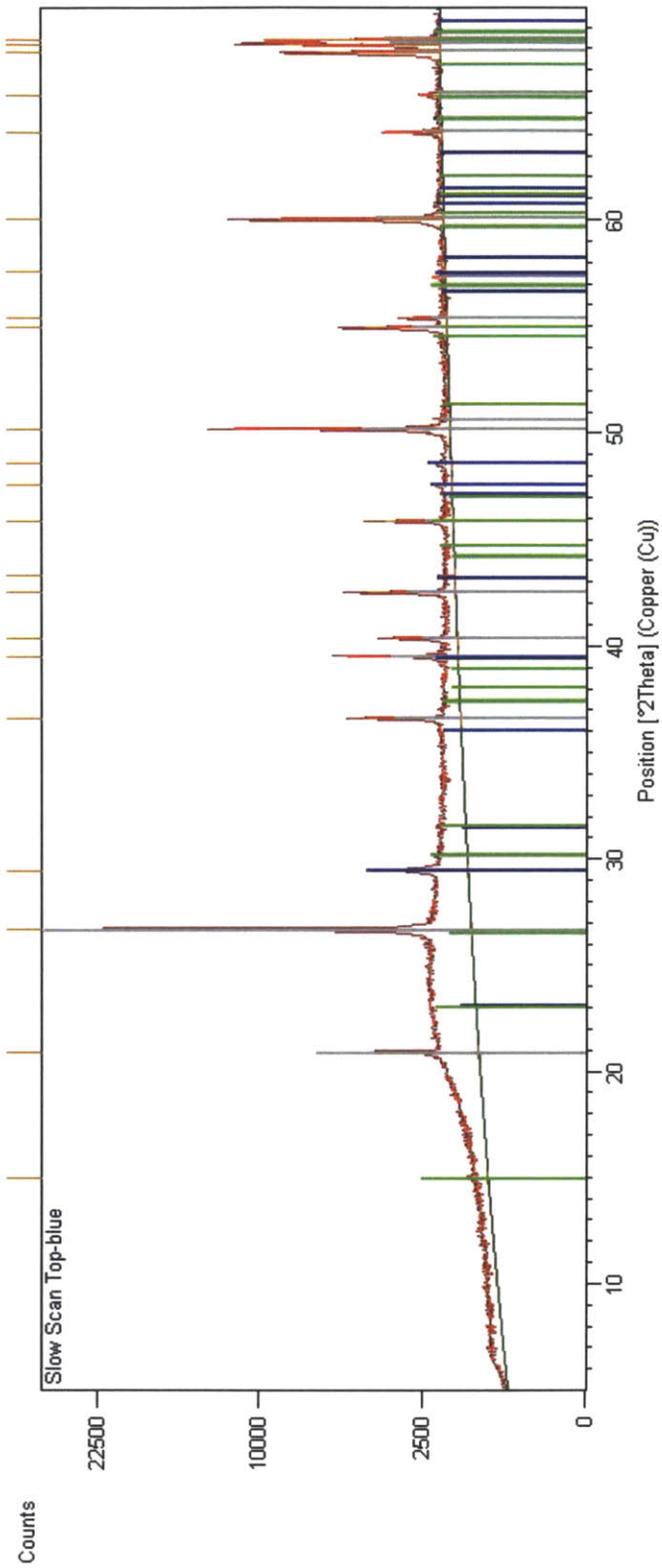

Figure 30: XRD Spectrum (with fitting) for the Top Blue Orientation.

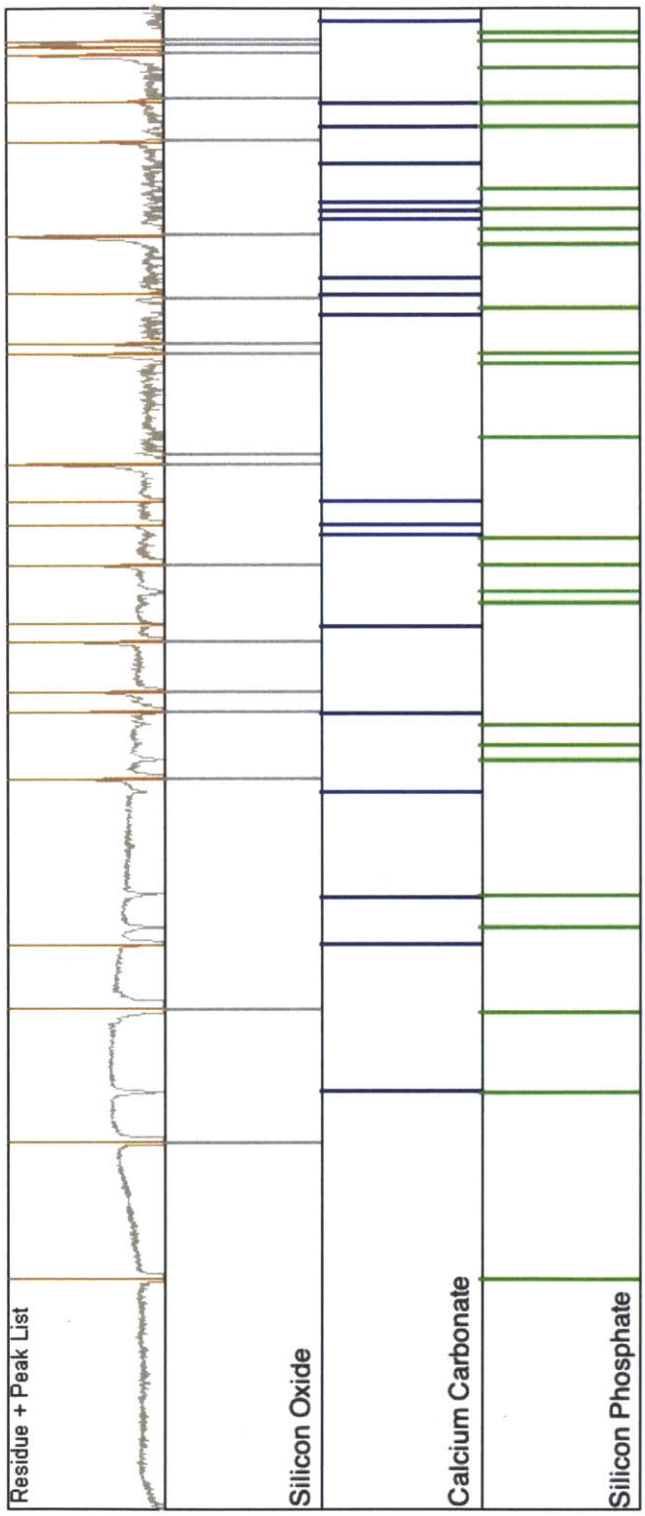

Figure 31: Labeled peaks for the Top Blue Orientation.

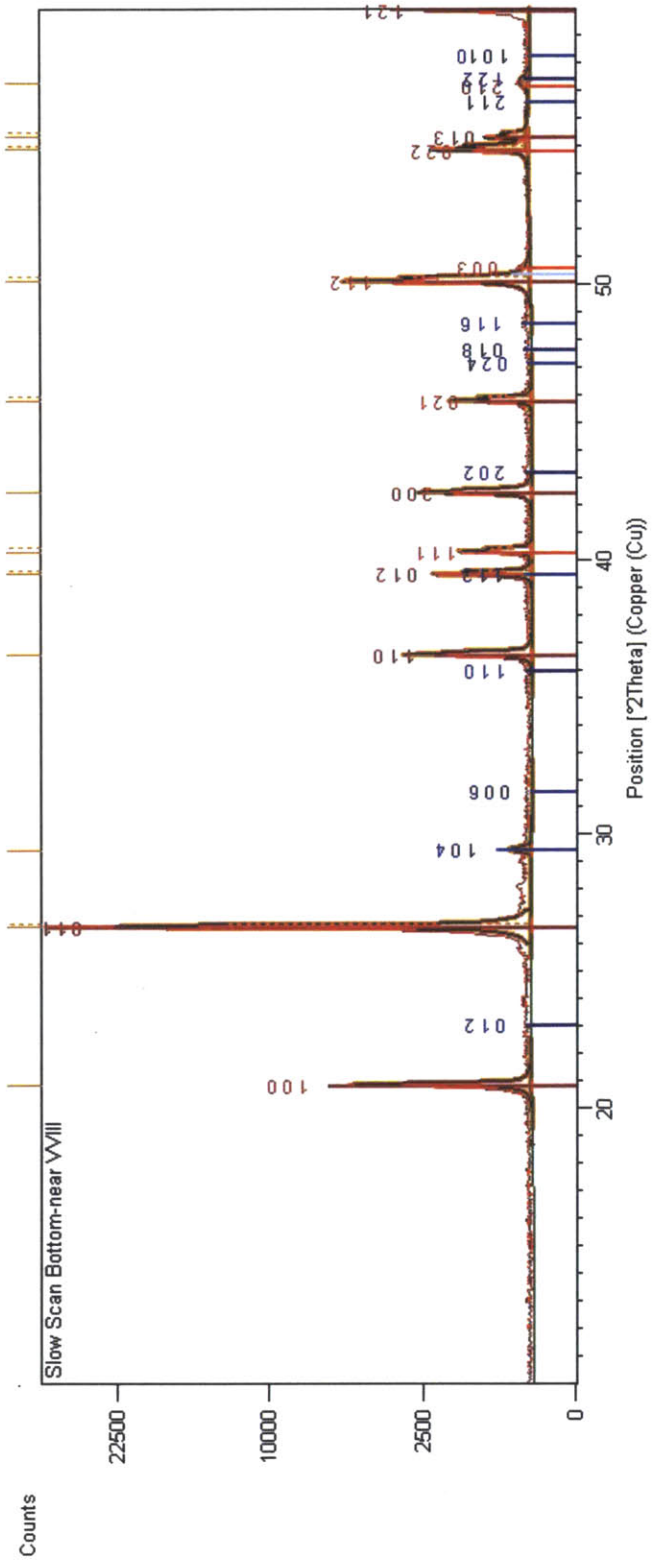

Figure 32: XRD Spectrum (with fitting) for the Bottom Near VVIII Orientation.

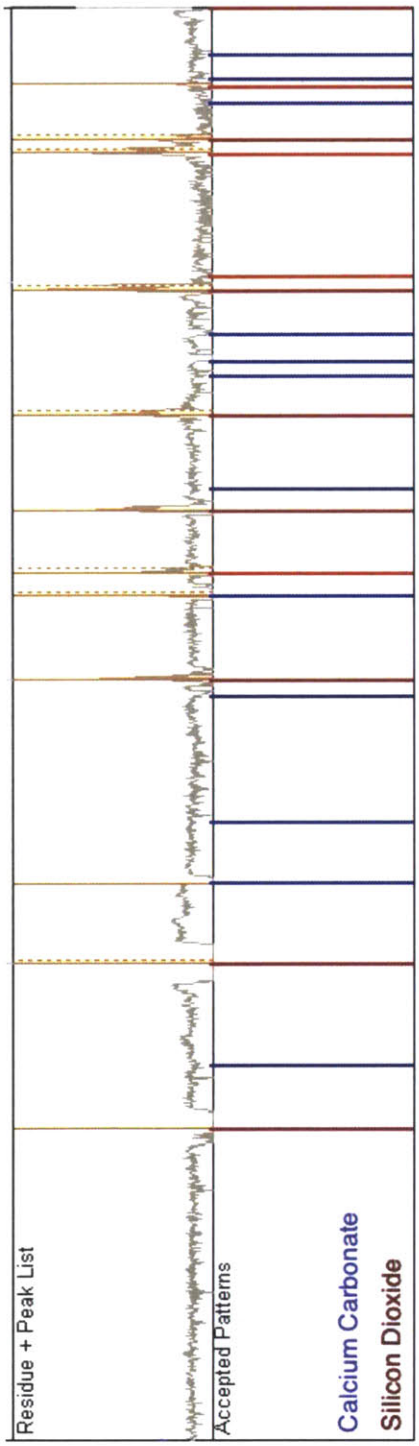

Figure 33: Labeled peaks for the Bottom Near VVIII Orientation.

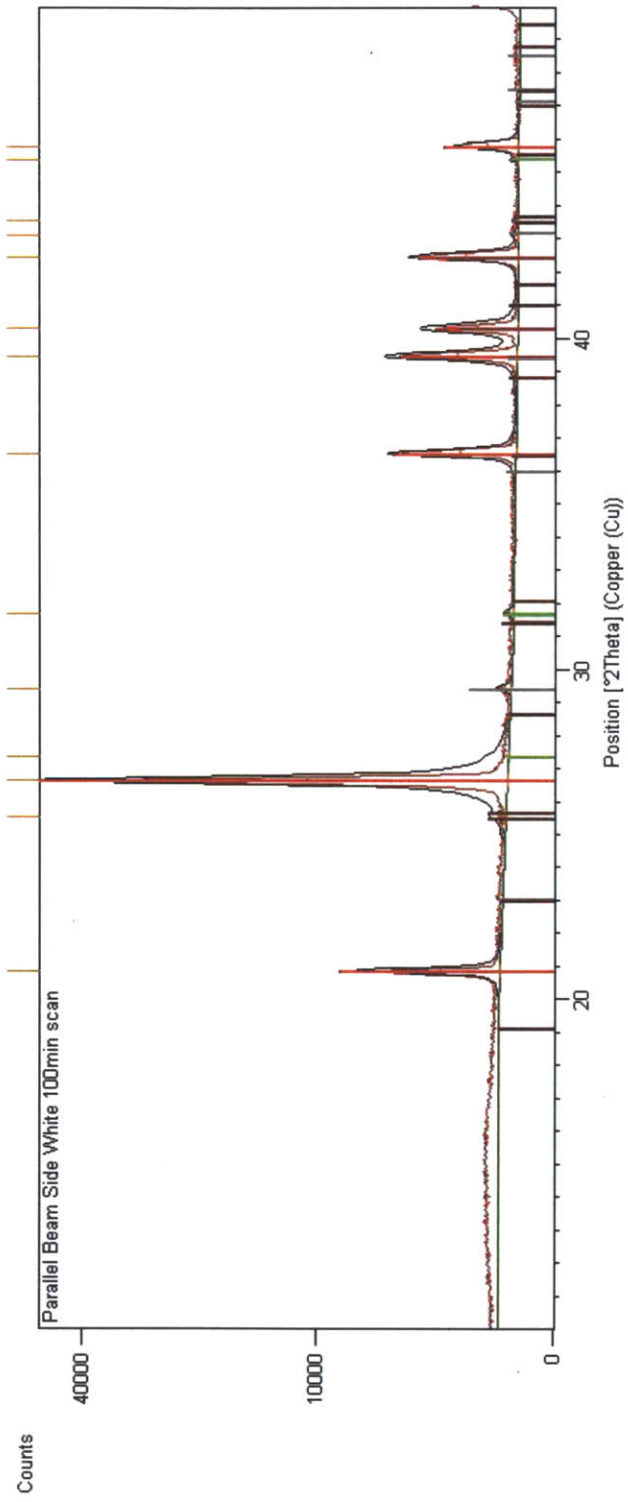

Figure 34: XRD Spectrum (with fitting) for the Side White Orientation.

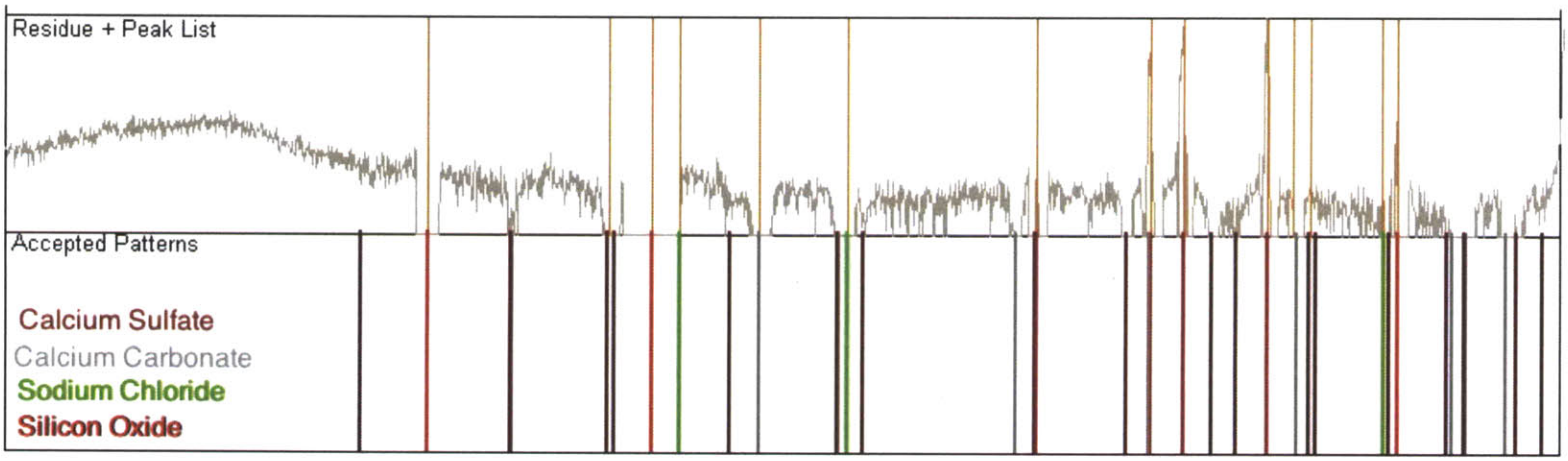
Residue + Peak List
Accepted Patterns
Calcium Sulfate
Calcium Carbonate
Sodium Chloride
Silicon Oxide

X-Ray Micro-Computed Tomography

The micro-CT analysis successfully generated a three-dimensional model of the Djoser faience tile. Several cross-sections of the tile were captured using this method, though no thin-section radiographs were produced before the computer used to reconstruct the data was damaged. Though these images are not available, the cross-sections do provide a view within the tile, as presented in Figure 36. The lighter areas correspond to lower densities while the darker areas correspond to higher densities. Some of the cross-sections, such as the one in Figure 36, reveal pores and voids within the tile as well as the nature of the hole that cuts through its back.

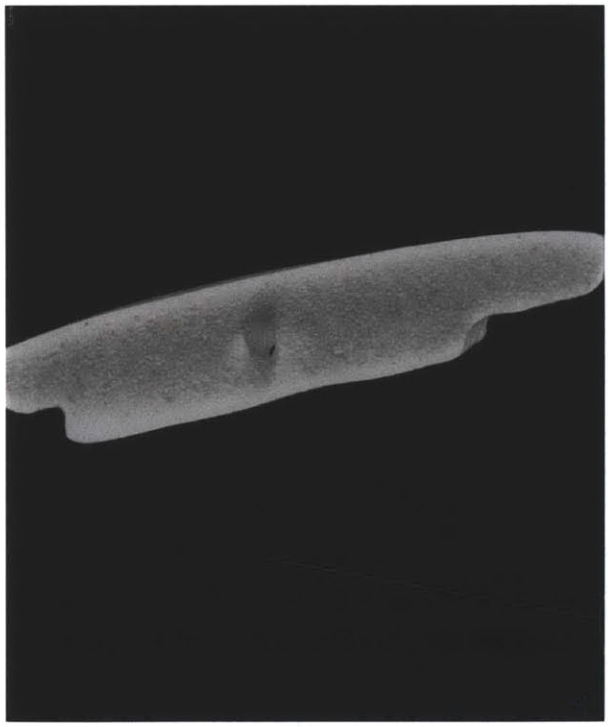

Figure 36: A cross-section of the Djoser faience tile using micro-CT.

Conclusions

Summary of Evidence

Based on these analyses, the Djoser faience tile studied is comprised of two components: a crystalline core and an amorphous glaze. Based on XEDS analysis supported by XRD analysis, the core is at least 98% quartz by atomic percentage with the remainder composed of calcium carbonate and some form of aluminum. In contrast, silicon dioxide composes 60.2% of the glaze by atomic percent. The remainder of the glaze contains calcium (19.7%), sodium (5.78%), copper (2.99%) and a variety of other cations as detailed in Tables 8 and 9 . Chloride anions are also present in the glaze and have previously been attributed to paratacamite (Manti, *et al.* 2008). Based on XEDS analysis, it appears that the chloride anions are most often associated with sodium cations in the form of NaCl. This result strengthens the case for the presence of the silicon phosphate phase observed in Figure 30.

Glazing Method

Of the three types of glazing (application, efflorescence and cementation), the most likely method used in the production of the Djoser faience tile was application based on XEDS analysis. Though the XRF analysis showed fairly consistent ranges of measurement, the shallow penetration depth and area-limiting features of XEDS analysis provided a more accurate comparison of glaze composition and core composition. While both phases exhibit high silicon content, the core does not appear to contain any copper or sodium and contains very little calcium as seen in Table 9. In contrast, the glaze

contains relatively high levels of both copper and sodium, as well as over 53 times the amount of calcium.

Since cementation glazing was not developed until far later than the Old Kingdom, the method of glazing would have been either efflorescence or application, assuming that this material was fired at high temperatures. As described earlier, those artifacts glazed by efflorescence exhibit consistent composition through the glaze and upper boundary layers. Since the XEDS measurements taken for the broken edge were collected just below the glaze-core interface, the compositions recorded appear to be too different to be the result of efflorescence glazing, assuming high temperature glass processing. In absence of comprehensive thin-section analysis, the differences in composition point to application as the most likely glazing method for the Djoser Step Pyramid faience tiles, assuming high temperature firing.

Evidence of Low Temperature Glazing

Several points of data throughout the analyses of data in the research described here lead back to the question regarding low temperature glaze formation. In the ESEM analysis of the Djoser faience tile, two types of crystal were visible on the tile's glazed surface as seen in Figure 19. The first of these crystals appears to be a non-melted piece of sodium chloride based on the results obtained through XEDS analysis. Since the melting temperature of sodium chloride is 801°C, the presence of non-melted pieces could suggest that the tile was not heated to such temperatures. The other crystal appears to contain calcium and carbon according to XEDS results. It is more difficult to correlate the carbon component with the calcium because carbon is present all over the surface of

the tile in the form of hydrocarbon residues, as is often the case when working with artifacts. According to the results obtained by the method of XRD, though, phases of calcium carbonate best completes the profiles produced by the Djoser faience tile in Figures 30, 32 and 34 instead of calcium hydroxide. The presence of calcium carbonate in the tile's glaze could indicate that it was not sufficiently heated to cause the transformation from calcium carbonate to calcium oxide, which occurs at 825°C.

Phosphorus Content

According to the work done by Davidovits and Davidovits, phosphorus has been thought to play a large role in the possible formation of glazes of Djoser Step Pyramid faience tiles approximately 600°C below the temperatures previously measured. These temperature results were obtained through reproductions glazed via efflorescence. According to XRD analyses, phosphorus is a likely component of the glassy network based on its presence in a crystalline phase detected on the glazed surface of the Djoser faience tile, though its lack of an RIR value made it impossible to determine its proportion in the crystalline phase. The ratio of phosphorus to silicon present in the Djoser faience tile studied here is as high as 0.015, from XRF data and approximately 0.0088 from XEDS data. In a study of iron-phosphate-glass conducted at the Pacific Northwest National Laboratory, the liquidus temperature (for glass formation) was measured to be within 10°C of 762°C, 92°C lower than earlier projections of faience glaze formation (Kim, *et al.* 2003). For their analysis, the relative atomic percent ratio of phosphorus to silicon was measured to be near 0.351. As this value is far above the measured value for the Djoser faience tile, the data indicate that the phosphorus content

of the glaze cannot adequately account for such a large decrease in glazing temperature. Phosphorus may play a role in the reduction of glazing temperature for conventional glaze firing, but its contribution cannot fully account for any substantial reduction in glaze melting temperature.

A Probable Last Option

While application glazing seems to be the most likely candidate assuming high glazing temperatures, it is not sufficient to account for a low temperature glazing process. A possible low temperature process for the production of Djoser faience tiles involves the presence of a soda-lime-silicate (likely hydrated) amorphous phase with copper absorbed in it. Based on XEDS analysis (supported by XRF analysis), the glaze of the tile contains a significant amount of copper (2.99% by atomic percent). According to the XRD analysis, there is no phase of crystalline copper present in the glaze. Since the entirety of the copper content must be in an amorphous phase, a copper-containing soda-lime-silicate glass is part of a process that could explain the glazing of Djoser faience tiles at low temperatures.

Future Research

In order to verify the method of glazing for the Djoser faience tiles, it will be necessary to perform thin-section analyses. Though such analysis had been planned using micro-CT methods, the device used was rendered inoperable before the results could be produced. Verifying the method of glazing will aid in experiments designed to reproduce these Egyptian faience tiles.

A more in-depth study of the crystals discovered in the glaze through ESEM analysis would reveal more information regarding the temperature of glazing. The sodium chloride crystals, if consistently un-melted throughout the entirety of the glazing process, could support the low temperature glazing hypotheses. Likewise, the presence of crystalline calcium carbonate supports the arguments for low temperature glaze production, though calcium hydroxide is known to undergo carbonation in the presence of carbon dioxide in the atmosphere (the process of lime mortar setting).

The most revealing compositional data in this study is the phosphorus data. Since the phosphorus does not adequately explain the temperature difference, it would be useful to perform a study of other elements detected in the specimen, such as chlorine and sulfur and their effects on silica glazes. Such investigations could involve the further use of XRF, ESEM and XEDS analyses for non-destructive purposes, but it may also be valuable to chip a small quantity of material from the sample (or several samples) for use in transmission electron microscopy (TEM) analysis, as had been initially planned for this analysis.

In the case of high temperature glazed faience, the objects created are held together by an amorphous component in the core. If the faience glazes at lower temperatures (below 250°C), this phase does not form. For low temperature glazed faience, one of the most important issues to resolve is to determine how the objects produced are held together.

Acknowledgements

I would like to thank Professor Linn Hobbs (DMSE, DNE; MIT) for his role as my thesis advisor and for obtaining the Djoser Step Pyramid faience tile analyzed in this thesis, as well as his suggestions to perform XRD, ESEM, XEDS and micro-CT analyses. I also would like to thank Dr. Scott Speakman for his suggestion of XRF analysis and his guidance during my XRF and XRD analyses.

I would like to thank Professor Heather Lechtman (DMSE, CMRAE; MIT) for her regular meetings and constant suggestions for improvement throughout my writing process.

I also would like to thank:
Dr. Joseph Davidovits (Geopolymer Institute)
Mr. Patrick Boisvert (CMSE; MIT)
Dr. David Bono (DMSE; MIT)
Dr. Neil Gershenfeld (CBA; MIT)
Ms. Nadya Peek (CBA; MIT).

Finally, I would like to thank the Undergraduate Research Opportunities Program for financial support of my research from the fall of 2010 to the summer of 2011.

References Cited

Clark, Robin and Peter J. Gibbs
1997 *Non-Destructive* In Situ *Study of Ancient Egyptian Faience by Raman Microscopy*. Journal of Raman Spectroscopy, Vol. 28, 99-103.

Crewe, L., E. Peltenburg and S. Spanou
2002 *Contexts for cruciform: the figurines of Chalcolithic Cyprus*. Antiquity 76.

Curators of the University of Missouri
2012 "Four Egyptian Faience Figures." Photo. MAA.missouri.edu 17 Apr. 2012. <http://maa.missouri.edu/exhibitions/1998/faience.html>.

Davidovits, Joseph and Ralph Davidovits
2004 *Why Djoser's blue Egyptian faience tiles are not blue? Manufacturing Djoser's faience tiles at temperatures as low as 250°C?*. IX International Congress of Egyptologists, Grenoble, France, September 6-11, Session 12.2.

Frame, Leslie, Donna Bright DeSordao, Yuan-Chi Chiang and Pamela Vandiver
2010 *Methods of Faience Manufacture in Antiquity: Investigation of Colorants and Technological Processes*. 2010 MRS Fall Meeting.

Kaczmarczyk, Alexander and Robert E.M. Hedges
1983 *The Elemental Composition of Faience Glazes*. Ancient Egyptian Faience: An Analytical Survey of Egyptian Faience from Predynastic to Roman Times, 20-139.

Kieffer, C. and A. Allibert
1971 *Pharaonic Blue Ceramics*. Archaeology, Vol. 24, 107-117.

Kim, D.-S., M.J. Schweiger, W.C. Buchmiller, J.D. Vienna, D.E. Day, D. Zhu, C.W. Kim, T.E. Day, T. Neidt, D.K. Peeler, T.B. Edwards, I.A. Reamer, R.J. Workman
2003 Iron Phosphate Glass as an Alternative Waste-Form for Hanford LAW. Pacific Northwest National Laboratory. February 2003.

Manti, P., P.T. Nicholson, A. Smith, M. Ellis, F. Mosselmans, T. Pradell and E. Pantos.
2008 The art and science of ancient Egyptian faience: the Step Pyramid tiles. Poster presented at *The Art of Hard Science*. STFC Daresbury Laboratory and Science and Heritage Program. Daresbury Laboratory, Warrington, 12 February 2008.

Metropolitan Museum of Art
2012a "Hippopotamus." Photo. Metmuseum.org 03 May 2012. <http://www.metmuseum.org/Collections/search-the-collections/100000444>.
2012b "Sphinx of Amenhotep III, possibly from a Model of a Temple." Photo. Metmuseum.org 03 May 2012. <http://www.metmuseum.org/Collections/search-the-collections/100000791>.
2012c "Grape Cluster from Cornice." Photo. Metmuseum.org 17 Apr. 2012. <http://www.metmuseum.org/collections/search-the-collections/100007901>.

National Palace Museum
2012 "Lapis Lazuli Miniature Mountain." Photo. NPM.gov.tw 17 Apr. 2012. <http://www.npm.gov.tw/exh96/Dazzling/descriptions09_en.html>.

Nicholson, Paul T. and E. Peltenburg
2000 *Egyptian Faience*. Ancient Egyptian Materials and Technology, 177-194.

Noble, JV
1969 *The Technique of Egyptian Faience*. American Journal of Archaeology, Vol. 73, 435-439.

Schiegel, S.
1988 Investigation on faience tiles from the walls of Djoser's south tomb in Saqqara: an approach to reveal the technique of their manufacture. *Vth Int. Congress of Egyptology, Cairo*. Abstract of Papers, 242-243.

Speakman, Scott
2011 Using the Bruker Tracer III-SD Handheld X-Ray Fluorescence Spectrometer using PC Software for Data Collection.

Tite, M.S.
1987 *Characterization of Early Vitreous Materials*. Archaeometry, Vol. 29, 21-34.

Tite, M.S. and M. Bimson
1986 *Faience: An Investigation of the Microstructures Associated with the Different Methods of Glazing*. Archaeometry, Vol. 28, 69-78.

Tyrrell, Johnna
2000 "Egyptian Scarab Seals, Back and Face." West Semitic Research Project. Photo. USC.edu 17 Apr. 2012. <http://www.usc.edu/dept/LAS/wsrp/educational_site/other_collections/annenberg/scarabs.shtml>.

Vandiver, PB and W. David Kingery
1986 *Egyptian Faience: The First High-Tech Ceramic*. High-Technology Ceramics: Past, Present, and Future, 19-34.